ENGINEERING OF
BIOMATERIALS
INŻYNIERIA BIOMATERIAŁÓW
JOURNAL OF POLISH SOCIETY FOR BIOMATERIALS AND FACULTY OF MATERIALS SCIENCE AND CERAMICS AGH-UST
CZASOPISMO POLSKIEGO STOWARZYSZENIA BIOMATERIAŁÓW I WYDZIAŁU INŻYNIERII MATERIAŁOWEJ I CERAMIKI AGH

Number 169
Numer 169
Volume XXVI
Rocznik XXVI

Year 2023
(Issue 2)
Rok 2023
(Zeszyt 2)

ISSN 1429-7248

PUBLISHER:
WYDAWCA:

Polish Society for Biomaterials in Krakow
Polskie Stowarzyszenie Biomateriałów w Krakowie

EDITORIAL COMMITTEE:
KOMITET REDAKCYJNY:

Editor-in-Chief
Redaktor naczelny
Elżbieta Pamuła

Editor
Redaktor
Patrycja Domalik-Pyzik

Secretary of editorial
Sekretarz redakcji
Design
Projekt
Katarzyna Trała

ADDRESS OF EDITORIAL OFFICE:
ADRES REDAKCJI:

AGH-UST
30/A3, Mickiewicz Av.
30-059 Krakow, Poland
Akademia Górniczo-Hutnicza
al. Mickiewicza 30/A-3
30-059 Kraków

Issue: 250 copies
Nakład: 250 egz.

Scientific Publishing House AKAPIT
Wydawnictwo Naukowe AKAPIT
e-mail: wn@akapit.krakow.pl

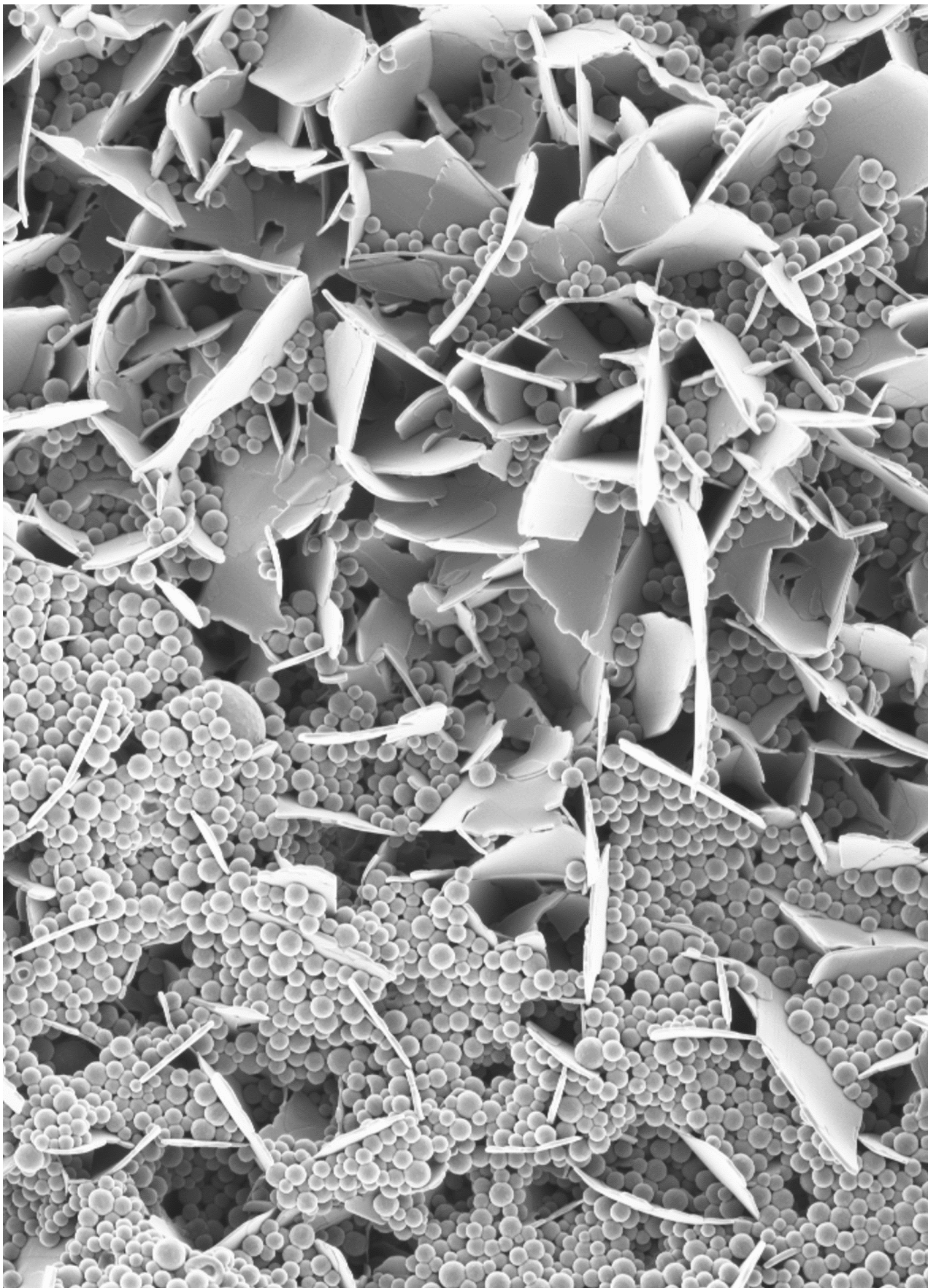

ENGINEERING OF BIOMATERIALS

EDITORIAL BOARD
KOMITET REDAKCYJNY

INTERNATIONAL EDITORIAL BOARD
MIĘDZYNARODOWY KOMITET REDAKCYJNY

ENGINEERING OF BIOMATERIALS

Wskazówki dla autorów

1. Prace do opublikowania w kwartalniku „Engineering of Biomaterials / Inżynieria Biomateriałów" przyjmowane będą wyłącznie w języku angielskim.
2. Wszystkie nadsyłane artykuły są recenzowane.
3. Materiały do druku prosimy przysyłać za pomocą systemu online (www.biomaterials.pl).
4. Struktura artykułu:
• TYTUŁ • Autorzy i instytucje • Streszczenie (200-250 słów) • Słowa kluczowe (4-6) • Wprowadzenie • Materiały i metody • Wyniki i dyskusja • Wnioski • Podziękowania • Piśmiennictwo
5. Autorzy przesyłają pełną wersję artykułu, łącznie z ilustracjami, tabelami, podpisami i literaturą w jednym pliku. Artykuł w tej formie przesyłany jest do recenzentów. Dodatkowo autorzy proszeni są o przesłanie materiałów ilustracyjnych (rysunki, schematy, fotografie, wykresy) w oddzielnych plikach (format np. .jpg, .gif., .tiff, .bmp). Rozdzielczość rysunków min. 300 dpi. Wszystkie rysunki i wykresy powinny być czarno-białe lub w odcieniach szarości i ponumerowane cyframi arabskimi. W tekście należy umieścić odnośniki do rysunków i tabel.
6. Na końcu artykułu należy podać wykaz piśmiennictwa w kolejności cytowania w tekście i kolejno ponumerowany.
7. Redakcja zastrzega sobie prawo wprowadzenia do opracowań autorskich zmian terminologicznych, poprawek redakcyjnych, stylistycznych, w celu dostosowania artykułu do norm przyjętych w naszym czasopiśmie. Zmiany i uzupełnienia merytoryczne będą dokonywane w uzgodnieniu z autorem.
8. Opinia lub uwagi recenzentów będą przekazywane Autorowi do ustosunkowania się. Nie dostarczenie poprawionego artykułu w terminie oznacza rezygnację Autora z publikacji pracy w naszym czasopiśmie.
9. Za publikację artykułów redakcja nie płaci honorarium autorskiego.
10. Adres redakcji:

Czasopismo
„Engineering of Biomaterials / Inżynieria Biomateriałów"
Akademia Górniczo-Hutnicza im. St. Staszica
Wydział Inżynierii Materiałowej i Ceramiki
al. Mickiewicza 30/A-3, 30-059 Kraków
tel. (48) 12 617 44 48, 12 617 25 61
e-mail: epamula@agh.edu.pl, kabe@agh.edu.pl

Szczegółowe informacje dotyczące przygotowania manuskryptu oraz procedury recenzowania dostępne są na stronie internetowej czasopisma:
www.biomaterials.pl

Instructions for authors

1. Papers for publication in quarterly journal „Engineering of Biomaterials / Inżynieria Biomateriałów" should be written in English.
2. All articles are reviewed.
3. Manuscripts should be submitted to editorial office through online submission system (www.biomaterials.pl).
4. A manuscript should be organized in the following order:
• TITLE • Authors and affiliations • Abstract (200-250 words) • Keywords (4-6) • Introduction • Materials and Methods • Results and Discussion • Conclusions • Acknowledgements • References
5. All illustrations, figures, tables, graphs etc. preferably in black and white or grey scale should be additionally sent as separate electronic files (format .jpg, .gif., .tiff, .bmp). High-resolution figures are required for publication, at least 300 dpi. All figures must be numbered in the order in which they appear in the paper and captioned below. They should be referenced in the text. The captions of all figures should be submitted on a separate sheet.
6. References should be listed at the end of the article. Number the references consecutively in the order in which they are first mentioned in the text.
7. The Editors reserve the right to improve manuscripts on grammar and style and to modify the manuscripts to fit in with the style of the journal. If extensive alterations are required, the manuscript will be returned to the authors for revision.
8. Opinion or notes of reviewers will be transferred to the author. If the corrected article will not be supplied on time, it means that the author has resigned from publication of work in our journal.
9. Editorial does not pay author honorarium for publication of article.
10. Address of editorial office:

Journal
„Engineering of Biomaterials / Inżynieria Biomateriałów"
AGH University of Science and Technology
Faculty of Materials Science and Ceramics
30/A-3, Mickiewicz Av., 30-059 Krakow, Poland
tel. (48) 12) 617 44 48, 12 617 25 61
e-mail: epamula@agh.edu.pl, kabe@agh.edu.pl

Detailed information concerning manuscript preparation and review process are available at the journal's website:
www.biomaterials.pl

STUDIA PODYPLOMOWE
Biomateriały – Materiały dla Medycyny
2023/2024

Organizator: Akademia Górniczo-Hutnicza im. Stanisława Staszica w Krakowie Wydział Inżynierii Materiałowej i Ceramiki Katedra Biomateriałów i Kompozytów **Kierownik:** prof. dr hab. inż. Elżbieta Pamuła **Sekretarz:** dr inż. Katarzyna Reczyńska-Kolman	**Adres:** 30-059 Kraków, Al. Mickiewicza 30 Pawilon A3, p. 208 lub p. 210 tel. 12 617 44 48, 12 617 23 38 email: epamula@agh.edu.pl; kmr@agh.edu.pl https://www.podyplomowe.agh.edu.pl/studia-podyplomowe-kursy-doksztalcajace-i-szkolenia/biomaterialy-materialy-dla-medycyny/
Charakterystyka: Tematyka prezentowana w trakcie zajęć obejmuje przegląd wszystkich grup materiałów dla zastosowań medycznych: metalicznych, ceramicznych, polimerowych, węglowych i kompozytowych. Słuchacze zapoznają się z metodami projektowania i wytwarzania biomateriałów a następnie możliwościami analizy ich właściwości mechanicznych, właściwości fizykochemicznych (laboratoria z metod badań: elektronowa mikroskopia skaningowa, mikroskopia sił atomowych, spektroskopia w podczerwieni, badania energii powierzchniowej i zwilżalności) i właściwości biologicznych (badania: *in vitro* i *in vivo*). Omawiane są regulacje prawne i aspekty etyczne związane z badaniami na zwierzętach i badaniami klinicznymi (norma EU ISO 10993). Słuchacze zapoznają się z najnowszymi osiągnięciami w zakresie nowoczesnych nośników leków, medycyny regeneracyjnej i inżynierii tkankowej.	
Sylwetka absolwenta: Studia adresowane są do absolwentów uczelni technicznych (inżynieria materiałowa, technologia chemiczna), przyrodniczych (chemia, biologia, biotechnologia) a także medycznych, stomatologicznych, farmaceutycznych i weterynaryjnych, pragnących zdobyć, poszerzyć i ugruntować wiedzę z zakresu inżynierii biomateriałów i nowoczesnych materiałów dla medycyny. Słuchacze zdobywają i/lub pogłębiają wiedzę z zakresu inżynierii biomateriałów. Po zakończeniu studiów wykazują się znajomością budowy, właściwości i sposobu otrzymywania materiałów przeznaczonych dla medycyny. Potrafią analizować wyniki badań i przekładać je na zachowanie się biomateriału w warunkach żywego organizmu. Ponadto słuchacze wprowadzani są w zagadnienia dotyczące wymagań normowych, etycznych i prawnych niezbędnych do wprowadzenia nowego materiału na rynek. Ukończenie studiów pozwala na nabycie umiejętności przygotowywania wniosków do Komisji Etycznych i doboru metod badawczych w zakresie analizy biozgodności materiałów.	
Zasady naboru: Termin zgłoszeń: od 20.09.2023 do 20.10.2023 (liczba miejsc ograniczona - decyduje kolejność zgłoszeń) Wymagane dokumenty: dyplom ukończenia szkoły wyższej Osoby przyjmujące zgłoszenia: prof. dr hab. inż. Elżbieta Pamuła (pawilon A3, p. 208, tel. 12 617 44 48, e-mail: epamula@agh.edu.pl) dr inż. Katarzyna Reczyńska-Kolman (pawilon A3, p. 210, tel. 12 617 23 38, e-mail: kmr@agh.edu.pl)	
Czas trwania: 2 semestry (od XI 2023 r. do VI 2024 r.) 8 zjazdów (soboty-niedziele) 1 raz w miesiącu przewidywana liczba godzin: 160	**Opłaty:** 3 000 zł (za dwa semestry)

32nd Biomaterials in Medicine and Veterinary Medicine

Annual Conference

12 – 15 October 2023 Rytro, Poland

SAVE THE DATE

12-15

OCTOBER

2023

www.biomat.agh.edu.pl

REGISTER

AND

SUBMIT

AN ABSTRACT

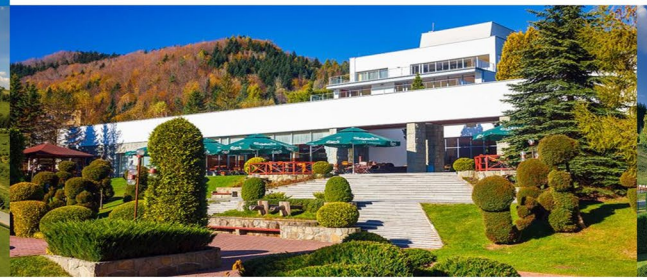

SPIS TREŚCI
CONTENTS

Wersja papierowa czasopisma „Engineering of Biomaterials / Inżynieria Biomateriałów" jest jego wersją pierwotną
Printed version of „Engineering of Biomaterials / Inżynieria Biomateriałów" is a primary version of the journal

PROTEIN RELEASE FROM DIFFERENT FORMS OF POLYLACTIDE AND ALGINATE COMPOSITE CARRIERS

Anna Morawska-Chochół*

AGH University of Krakow,
Faculty of Materials Science and Ceramics,
Department of Biomaterials and Composites,
al. A. Mickiewicza 30, 30-059 Krakow, Poland
*e-mail: morawska@agh.edu.pl

Abstract

The development of composite biomaterials constituting both a porous scaffold for filling tissue defects (especially bone tissue) and a carrier of biologically active substances (proteins) is an innovative approach of the presented research. The paper presents the following studies of obtained composites: model protein (bovine serum albumin, BSA) release, changes in microstructure during incubation and bioactive potential in a simulated biological environment (based on scanning electron microscopy with X-ray microanalysis – SEM/EDS – and infrared spectroscopy – FTIR). Three types of composites with a poly(L-lactide) matrix PLLA were investigated. PLA fibres covered with silica-calcium sol, calcium alginate fibres and calcium alginate beads were used as modifiers of the PLA matrix and carriers of protein. Process of releasing albumin proceeded differently depending on the material and form of the carrier. In the case of calcium alginate fibres, almost all protein was released within 14 days. For the remaining materials, this amount was reached after 3 weeks. All tested composites showed bioactive potential connected with apatite precipitation during incubation in a simulated biological environment. However, coating PLA fibres with silica-calcium sol significantly increased this effect. The highest cell viability was observed for a biomaterial modified by calcium alginate beads.

Keywords: *polylactide, calcium alginate, bovine serum albumin, protein release, bioactive composite, multifunctional composites*

Introduction

Due to trauma in life, regeneration of lost tissue such as bone, cartilage, skin, muscle, and tendons is still an actual problem. Grafts for filling large defects are one of the ways to heal and regenerate tissue [1,2]. Scaffolds which can deliver biologically active reagents stimulating growth of the treated tissue are a new conception [3]. This solution must combine a surgical implant with a drug carrier. Such a complex function increases the requirements for this type of biomaterial. On the one hand, it must perform a structural function, allowing the restoration of natural biomechanics thanks to appropriate mechanical parameters, and during the healing time undergo controlled degradation, allowing overgrowth of tissue through the implant. On the other hand, proper biological action is desirable, serving to activate and stimulate regenerative processes by providing the appropriate proteins, growth factors, enzymes, or drugs. The most popular materials for the delivery of biologically active substances are degradable polymers, such as polylactide and alginate [4-6]. Alginates are immensely popular hydrogels due to their biocompatibility, similarity to the natural extracellular matrix, high swelling capacity and low costs of production. However, too fast diffusion of the delivered drug is often a problem in alginate carrier application [7]. The controlled release can be realized by chemical modification of alginate beads by hydrophobic materials in the form of a coating or incorporation of organic compounds into alginate beads to create a hydrophobic gel matrix [7]. The poor mechanical parameters of alginate significantly limit the possibilities of their application.

Polylactides (PLAs) are also popular materials in drug delivery. Common forms in these applications are nano- and microcapsules or nonwovens [6,8-10]. Their only function is the controlled delivery of biologically active agents, and mechanical stabilization cannot be realized. Other forms of PLAs, such as fibres or scaffolds, are also being developed in the current research [11-13]. PLA and its copolymers, thanks to relatively good mechanical parameters and the ability to control the time of their degradation, are widely used as scaffolds in tissue engineering. The desired scaffolds microstructure can be controlled by selecting the appropriate technology (electrospun mats, 3D printing, freeze-drying) [14-16]. The creation of PLAs-matrix composites also allows them to be strengthened mechanically (especially by fibre modification) and gives them additional properties, such as bioactivity (hydroxyapatite or bioglass additives for healing of bone defects) [16,17]. Such properties are particularly important in the case of grafts intended to fill bone tissue defects. Bone tissue is characterized by a high regenerative potential, but in the case of extensive cavities the use of implants is required, temporarily replacing its functions.

The original approach of the present work is the connection of a scaffold and a carrier of biologically active substances by placing the carrier in the form of beads or fibres in a PLA matrix to decrease the rate of protein release. The new conception of this paper is creating multifunctional composite materials able to deliver protein and also to fulfil a mechanical (constructional) function, with the proper porosity for cell migration and proliferation, and with bioactive potential. Its application to filling extensive tissue defects would give the possibility for delivery of drugs, growth factors, or other biologically active proteins (reagents). This aim was realized by creation of the novel composite materials, in which protein was incorporated in the fillers of the PLA matrix, such as PLA and alginate fibres or alginate beads. The influence of the type of polymeric carrier (fillers), their form, and the way of protein connection on albumin release were investigated. Bovine serum albumin (BSA) was applied as a model protein, a common approach in the literature [6,18,19]. Moreover, BSA gives great potential for binding reactive groups of the other compounds thanks to the free sulphydryl groups existing in the peptide chain [20]. The bioactive potential and biocompatibility of the proposed composites were also evaluated.

[Engineering of Biomaterials 169 (2023) 2-10]

doi:10.34821/eng.biomat.169.2023.2-10

Submitted: 2023-06-28, Accepted: 2023-07-19, Published: 2023-07-22

Materials and Methods

Materials

The following materials and reagents were used in the preparation of the composite samples: poly-L-lactide PLLA – Ingeo™ 3051D, NatureWorks® LLC (glass transition temperature Tg 55-65°C, molecular weight Mn 61000 g/mol, polydispersity 1.5); long poly-L-lactide fibres (fibre diameter 9.6 μm, tensile strength 1.34 GPa, Young's modulus 20.1 GPa, ε_{Fmax} 30.2%) and long calcium alginate fibres (fibre diameter 10.65 μm, tensile strength 261 MPa, Young's modulus 15.1 GPa, ε_{Fmax} 1.7%) – obtained by the wet solution method at the Department of Material and Commodity Sciences and Textile Metrology of Lodz University of Technology in Poland (the process of manufacturing fibres and their parameters are described in a previous paper [21]); bovine serum albumin (BSA) – Sigma-Aldrich; culture medium – high-glucose DMEM (4.5 g/l) with L-glutamine (Sigma-Aldrich); dichloromethane CH_2Cl_2 (Poch S.A.); TEOS (Sigma-Aldrich); 1 mol $Ca(NO_3)4H_2O$ (Sigma-Aldrich); sodium alginate (Sigma-Aldrich); $CaCl_2$ (Poch S.A.); phosphate-buffered saline – PBS (Sigma-Aldrich).

Spherical beads with BSA (1.29 mm in diameter) were formed by forcing the flow of 6% sodium alginate sol containing 1.5% BSA solution from the needle (0.5 mm) and gelling them in the 10% $CaCl_2$ solution [21].

Sample preparation

Three types of composite carriers of BSA were obtained according to the procedure described in an earlier paper [21]: (1) PPA – PLA matrix modified with PLA fibres (40 wt.%; fibres covered by protein), (2) PAA – PLA matrix modified with alginate fibres (40 wt.%; fibres covered by protein), (3) PKA – PLA matrix modified with protein-loaded alginate beads (20 wt.%).

Test methods

pH and conductivity of incubation fluids

pH and conductivity measurements were performed for 8 weeks on water extracts during incubation of the tested materials at 37°C in distilled water (DW). Before measurement, the extracts were cooled to room temperature. A CP-411M Elmetron microcomputer pH meter was used to measure pH, and a CC-315 Elmetron conductivity meter equipped with an EC-60 Elmetron electrode was used to measure conductivity.

In vitro BSA release

The samples were incubated in PBS of pH = 7.4 at 37°C for 3 weeks. A constant ratio of sample mass to PBS volume was maintained (1 g/25 ml). The *in vitro* BSA release was determined using the following steps. After a certain time, 5 ml of the supernatants were taken for testing and replaced by a fresh 5 ml of PBS. The BSA concentration of the sampled solution was determined by using a UV-vis spectrophotometer (CECIL CE2502). The absorbance was monitored at 280 nm [22,23]. The BSA concentration was calculated using a calibration curve created by known BSA concentration solutions. All samples were analysed in triplicate and expressed as the mean ± standard deviation. The value of $p < 0.05$ was regarded as statistically significant.

Microstructure and element analysis (SEM and EDS)

The samples' microstructure was determined by using a scanning electron microscope (SEM; FEI Nova NanoSEM, USA). The elements were analysed by using an X-ray energy dispersion (EDS) microanalyser coupled with a microscope. Samples were sprayed with carbon before analysis. The tests were performed for initial samples and after 4 weeks of sample incubation in PBS (pH = 7.4) and DW at 37°C.

FTIR analysis

To determine the structural changes occurring during the incubation of composites in a simulated biological environment, the initial samples and samples after 4 and 8 weeks of incubation in PBS (pH 7.4, 37°C) were examined by Fourier transform infrared spectroscopy (FTIR). The research was carried out using the transmission technique in KBr using a Bio-Rad FTS60v spectrometer. FTIR spectra were recorded in the mid-infrared in the range of 4000-400 cm^{-1}.

Cell viability assay

Determination of cell viability on the samples' surface was conducted in primary culture of human osteoblasts (NHOst; Lonza, USA). The cells were grown in plastic bottles (Nunclon, Denmark) in OGM BulletKit culture medium (Lonza, USA) with 10% calf serum FBS, in an atmosphere of 5% CO_2 and temperature of 37°C in a HeraCell incubator (Heraeus, Thermo Scientific, Germany). Cells from passage 5 were used in the culture. The cell suspension was obtained by adding 5% trypsin from EDTA (Lonza, USA). After flushing and centrifugation, the cells were brought to a concentration of 1.5×10^4 cells/ml, after which 1 ml of cell suspension was placed in wells of a 48-well culture plate (Nunclon, Denmark) containing sterile samples with a diameter of 11 mm. The positive control was the polystyrene of the bottom of the wells of the culture plate (TCPS). NHOst cell culture was carried out for 3 and 7 days. After allotted time, the cells growing on the surface of the samples were subjected to a viability test (CellTiter test), and the morphology of the cells in an optical fluorescence microscope was evaluated (Olympus, Japan). Cell tests were performed at the Faculty of Pharmacy at Jagiellonian University, Medical College in Poland.

Results and Discussion

The results of the measurements of the amount of albumin released are presented in two graphs covering the period of the first 24 hours (FIG. 1a) and the period from the first day to 3 weeks (FIG. 1b). Significant changes were observed already within the first day of incubation, especially for PPA composite, when about 29% of the concentration of the introduced protein was reached. Such a significant rate of release in the initial stage of incubation compared to other composites is because BSA was absorbed only on the surface of the fibres. In the case of alginate fibres, as a result of their swelling in the aqueous environment, protein could also be connected inside the fibres. After 2 days of PPA incubation, protein release had a linear course. These studies show that the silica–calcium sol coating does not block BSA release from PLA fibres.

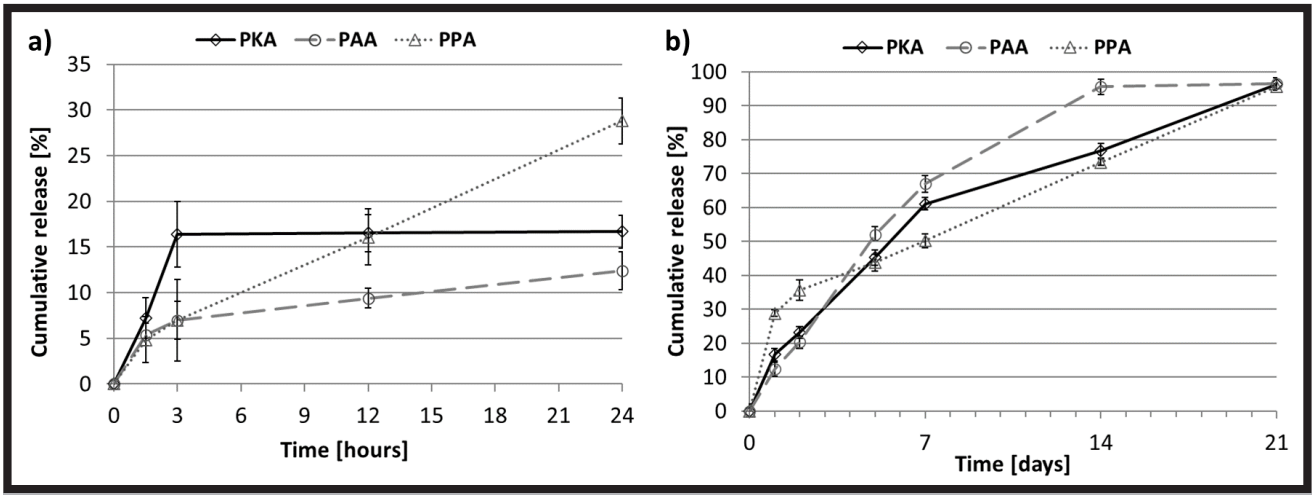

FIG. 1. Release of BSA from composites: a) during 24 h, b) during 3 weeks of incubation in PBS.

For PKA, about 17% of BSA was reached already within the first 3 hours of incubation. During the first day, the release was the slowest in the case of the PAA composite, where after 24 hours the albumin concentration was only 12%. The observed changes indicate that despite the stability of the individual phases of the composite, especially the matrix, the release of albumin begins immediately after the samples are placed in the aqueous environment. Release of albumin from the fibres' surface or alginate beads is possible thanks to the ability of the PLA matrix to absorb water and then migration of albumin in the PLA structure [24]. The rate of albumin release in the first stage of incubation can also be related to the composite's porosity and the character of PLA/modifier interfaces, which fulfil diffusion of the incubation medium and albumin (FIGs 2 and 3) [25].

The maximum protein concentration was reached after 3 weeks of incubation for all tested composites (FIG. 1b). This was confirmed by EDS analysis of the samples. In the case of the initial composites, a signal from nitrogen and sulphur from the protein was visible on the modifier's surface (FIG. 2). However, these elements were not identified after 4 weeks of incubation in PBS (FIG. 3).

Absorbance measurements showed that the rate of BSA release decreases gradually with incubation time. For alginate-carrier composites (PKA and PAA), the first stage of intensive release includes up to 1 week of incubation, during which approx. 67% of the maximum albumin content in PAA and approx. 61% of the content in PKA are released into the supernatant. For PAA, the release is the fastest, and after 2 weeks of incubation, almost the maximum concentration of the introduced protein is achieved (approx. 96%). This is due to the easier penetration of fluids through the fibre-matrix interfaces because of alginate fibres swelling and moving. The changes in alginate fibre morphology are visible in the SEM image after 4 weeks of incubation in PBS (FIG. 2b and FIG. 3b). Moreover, numerous pores can be observed. Compared to the number of pores in the initial composite, it can be seen that their number and size increased significantly after incubation. This indicates the gradual degradation of the fibres and their movement.

In the case of PKA, the protein was released gradually from hydrogel beads swelling under the influence of incubation. As shown by studies of the kinetics of BSA release from calcium alginate beads described by Nochos et al., the greater the ability to swell, the faster the BSA release process takes place [26]. This results from physical entanglements between the protein and alginate chains. At pH 7.0, alginate is in the form of a polyanion, and albumin is negatively charged; therefore, electrostatic interactions are not expected [27]. The PLA matrix hinders the swelling of alginate beads during the initial stage of incubation. On the other hand, because of drying of PKA composites, capsule shrinkage and delamination at the interface are visible in the SEM photo after 4 weeks of incubation (FIG. 3c). Unlike fibre modifications, in the case of beads, their interfaces with the matrix do not make contact with the surface of materials. Therefore, the diffusion of fluid into the interior of the composite and BSA into the incubation medium can take place mainly through the structure of the PLA matrix.

A common problem in the use of alginate carriers is too rapid release of delivered substances to the surrounding environment [7,28]. The solution proposed in this work, consisting in placing the carrier in the form of beads or fibres in the PLA matrix, effectively allows a reduction in the rate of release of the model protein. At the same time, the implant designed in this way can also perform other functions, such as a mechanical one and as a scaffold for regenerated tissue, stimulating its growth by delivering protein. As demonstrated in previous work, these composites are characterized by satisfactory mechanical properties for filling bone defects and favourable porosity due to the possibility of cell proliferation [21]. In particular, the PPA composite is characterized by a very attractive microstructure similar to that of trabecular bone (FIG. 2c). The proposed composites can be used in a situation where long-term release of the active substance is required in the treatment process.

Most apatite secretions with stoichiometry similar to that of biological apatite can be observed after 4 weeks of incubation in PBS of the PPA composite (Ca/P is 1.53) (FIG. 3a). This indicates the significant role of silica-calcium sol covering PLA fibres in the process of nucleation and growth of apatites, thus this composite has the greatest bioactive potential. EDS analysis showed the presence of silicon in the precipitates, which may suggest its incorporation into the structure and role in inducing the process of their formation. The presence of calcium phosphates was additionally confirmed by the analysis of FTIR spectra (FIG. 4), where on the PPA spectra after 4 and 8 weeks of incubation in PBS, the bands associated with vibrations of $PO4^{3-}$ groups in the range of 560-600 cm^{-1} are visible [29]. The most intense bands of phosphate groups in the range of 1020-1100 cm^{-1} overlap the C-O-C bands of PLA. However, an increase in the intensity of bands in this range after incubation compared to the spectrum of initial PPA is visible. This confirms the presence of numerous apatite secretions in the composite.

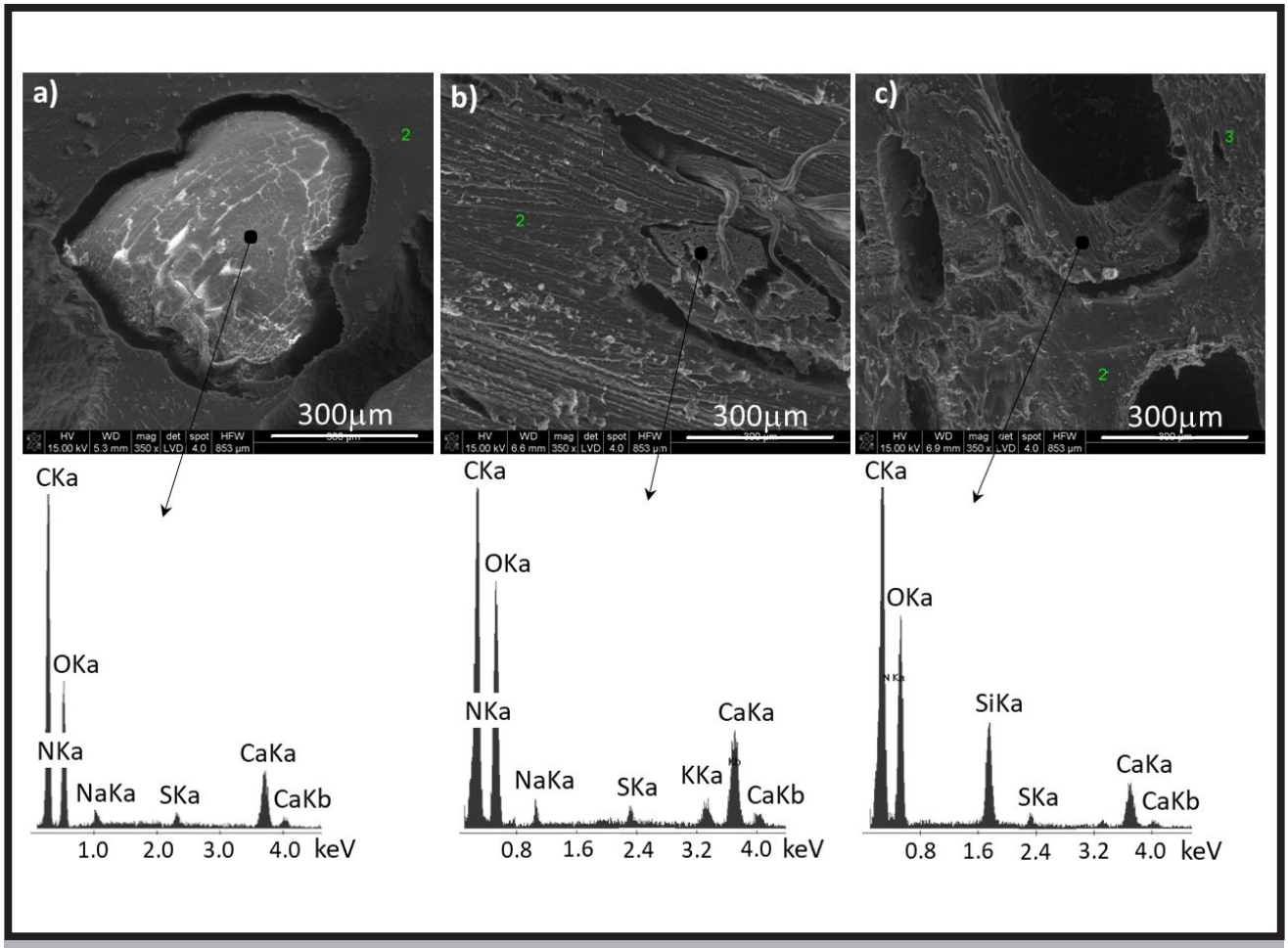

FIG. 2. SEM microstructure and EDS analysis of initial composites: a) PKA, b) PAA, c) PPA.

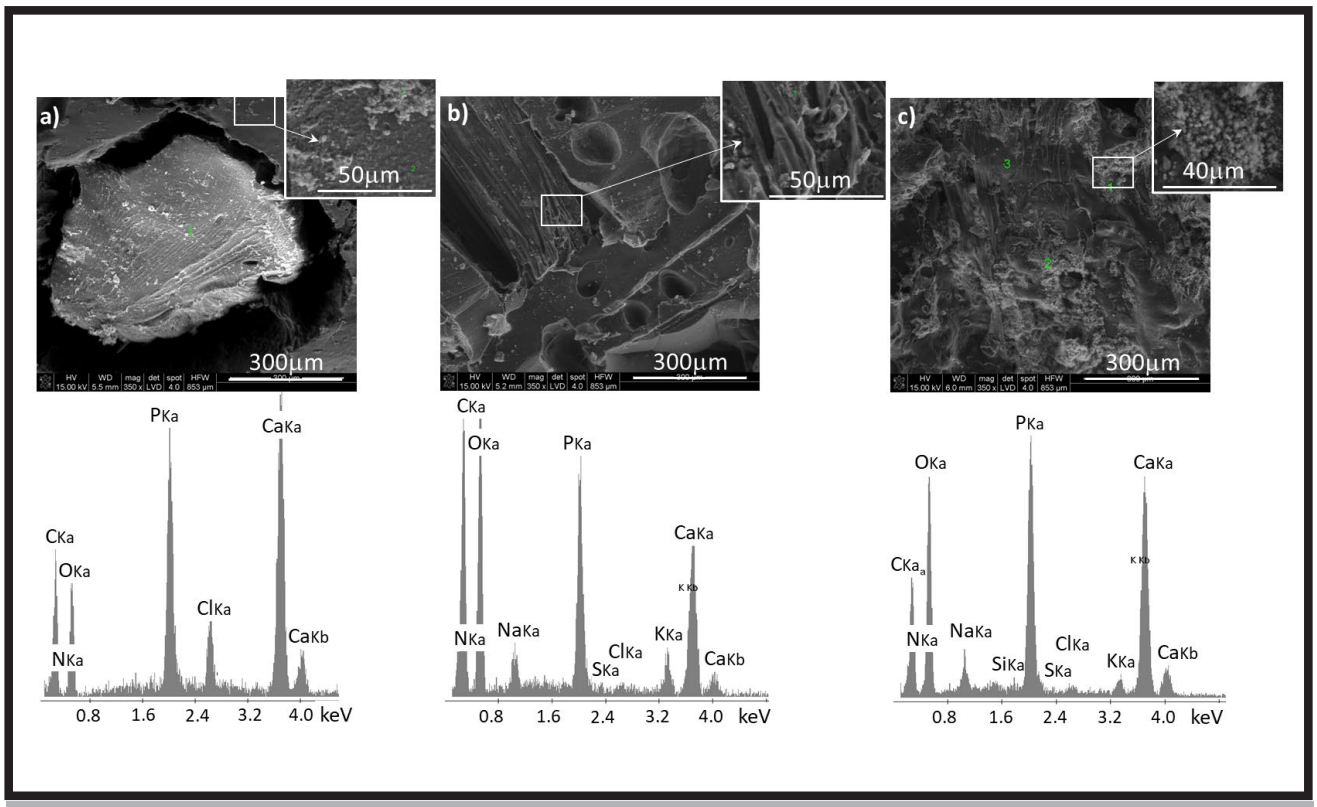

FIG. 3. SEM microstructure and EDS analysis of composites after 4 weeks of incubation in PBS: a) PKA, b) PAA, c) PPA.

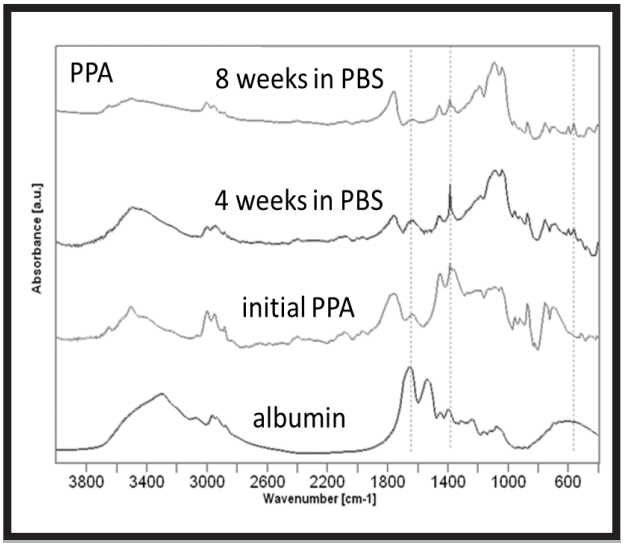

FIG. 4. FTIR spectra of albumin and PPA composite: initial and after 4 and 8 weeks of incubation in PBS.

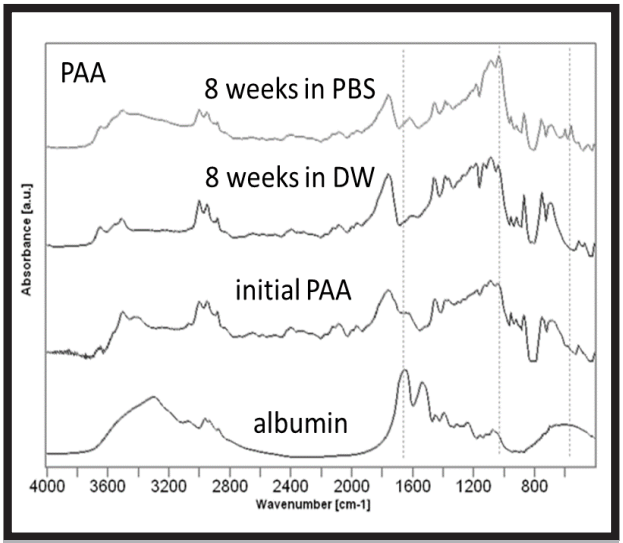

FIG. 5. FTIR spectra of albumin and PAA composite: initial and after 8 weeks of incubation in distilled water (DW) and PBS.

Importantly, calcium phosphate precipitations were present on the surface of the PAA composite after 4 weeks of incubation in PBS, although not as numerous as were visible in the case of the PPA composite (FIG. 3a). The presence of apatite was confirmed by elemental analysis. However, the molar ratio of calcium to phosphorus was 1.29 and slightly different from that typical for biological apatite (1.5-1.67). A small amount of sulphur may result from the adsorption of the released protein on the surface of the composite.

SEM images of the PKA composite after 4 weeks of incubation in PBS also allowed the observation of clearly visible calcium phosphate precipitation on the surface of the composite (FIG. 3c). Elemental analysis showed the presence of calcium to phosphorus in a ratio of 2.33, which is probably related to the increased amount of calcium derived from alginate beads.

FIGs 5 and 6 show the FTIR spectra of the PAA and PKA composites after 8 weeks of incubation in DW and PBS. No changes were observed on the spectra that could indicate degradation of PLA. However, the disappearance of the band correlated with albumin (amide I at approx. 1650 cm^{-1}), which is associated with its release (incubation in DW and PBS), can be observed. Moreover, the presence of bands connected with the $PO4^{3-}$ groups in the range of 560-600 cm^{-1} on spectra obtained for composites after incubation in PBS indicates the presence of apatite secretions. Alginate-derived bands are difficult to interpret due to the overlap of PLA and albumin bands, but after 8 weeks of incubation, the band at approx. 1620 cm^{-1} can be associated with vibrations of carboxyl groups -COOH in alginate.

The *in vitro* stability of the tested composites (especially modifiers) and the influence of modifying phases on the water environment were assessed on the basis of pH and conductivity changes of DW (FIG. 7). The measurements did not show any significant changes in pH that could indicate that the PLA degradation process had begun. This indicates that the matrix of the composites is stable in the aqueous environment during the test period (8 weeks of incubation). These results confirm previous studies on PLA degradation (PLA with the same chemical structure), which have shown that the degradation process of this polymer begins after approximately 15 weeks of incubation in DW [30].

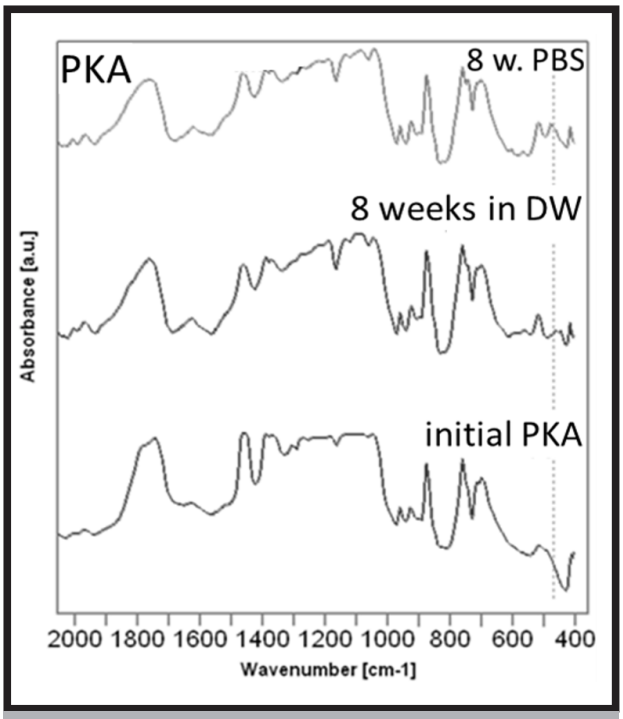

FIG. 6. FTIR spectra of PKA composite: initial and after 8 weeks of incubation in distilled water (DW) and PBS.

Despite the lack of significant changes in the pH of the supernatants, there was a visible change in their conductivity after the first day of incubation, especially in the case of the PKA and PPA composites. In the case of the PKA composite, the largest increase in conductivity occurred during the first 7 days, then the changes were gradual up to 8 weeks of incubation. As shown by the results presented above, the release of albumin occurs up to 3 weeks of incubation; therefore, an increase in conductivity after this time can be associated with partial degradation of calcium alginate. This is confirmed by the clearly smaller size of the beads visible in the SEM photo after 4 weeks of incubation in DW (FIG. 8a).

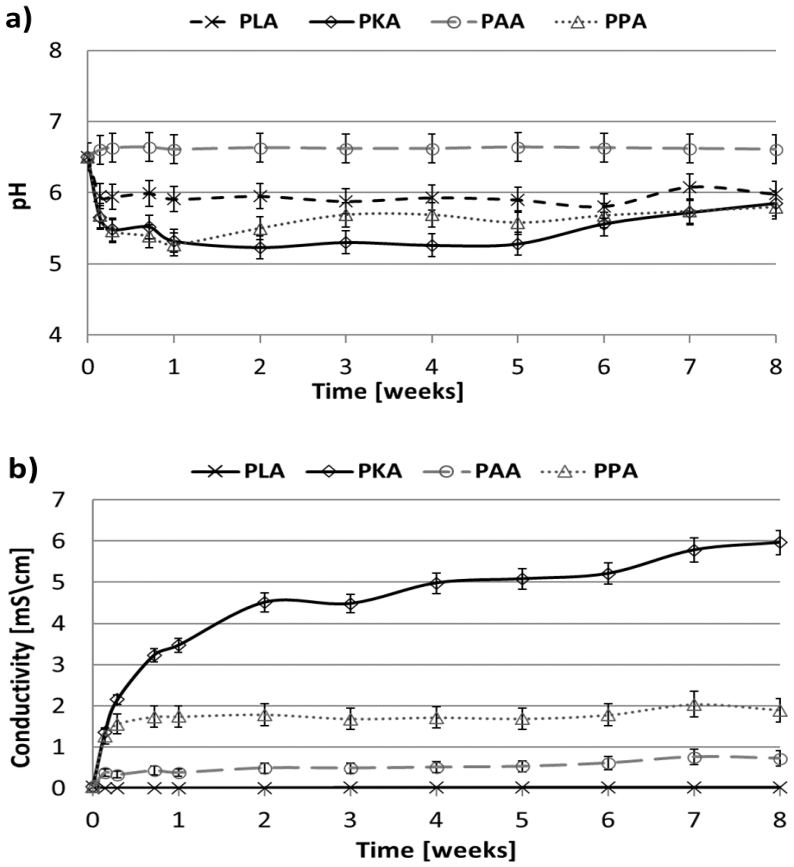

FIG. 7. Changes of pH (a) and conductivity (b) of distilled water during incubation of composites.

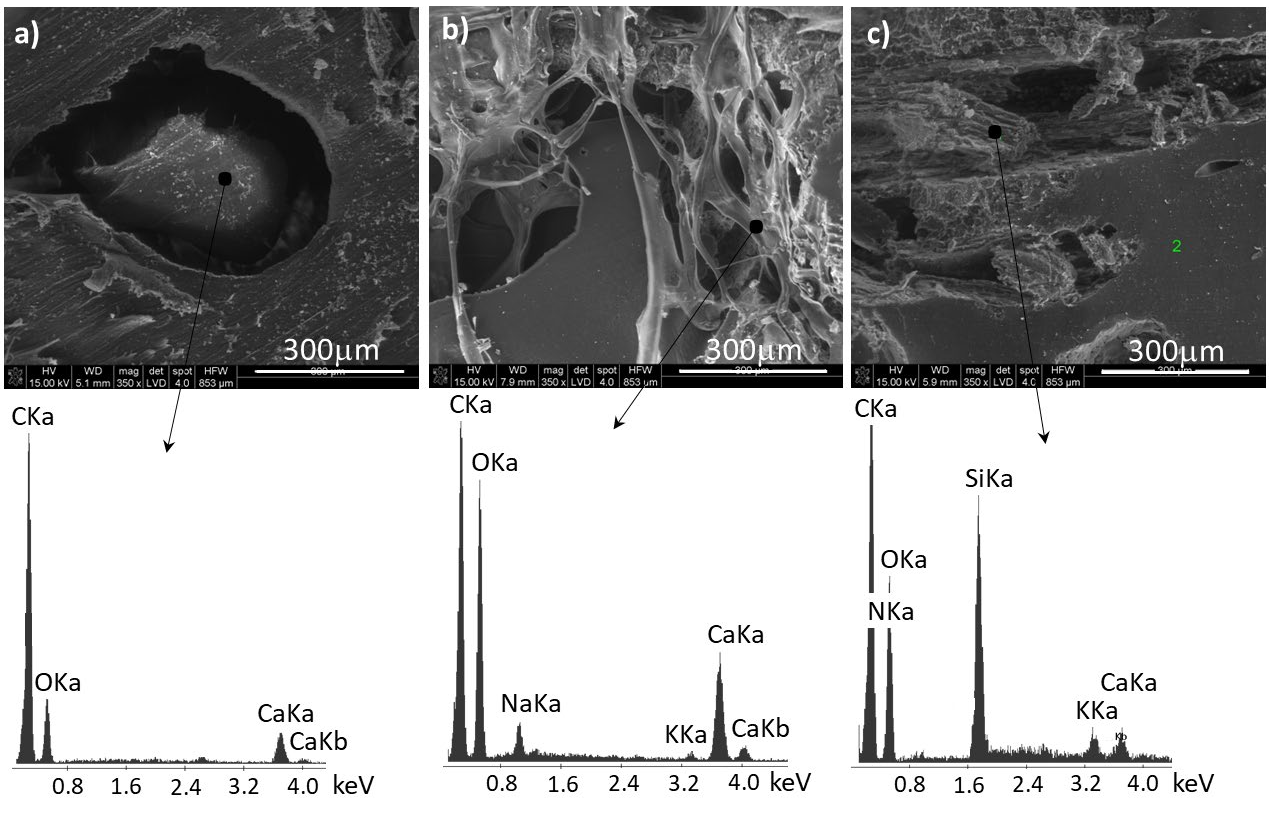

FIG. 8. SEM microstructure and EDS analysis of composites after 4 weeks of incubation in distilled water: a) PKA, b) PAA, c) PPA.

The same applies to the PPA composite. The greatest increase in conductivity occurred already on the first day of incubation, after which these changes were no longer so intense. This is largely associated with the intense release of albumin during this time: after the first day, 29% of the introduced protein was achieved (FIG. 1). In the case of the PPA composite, the increase in conductivity is associated not only with the release of albumin, but also with decomposition and release of the silica-calcium sol components. This conclusion was confirmed by the EDS analysis performed in the outer part of the fibre after 4 weeks of incubation in DW (FIG. 8c), which showed different proportions of silicon and calcium than in the sample before incubation (FIG. 2c). Importantly, the high content of silicon after 4 weeks of incubation may indicate its incorporation into the structure of the material. Moreover, the fragmentation of PLA fibres is visible in SEM images after this time. Such a rapid degradation process may be related to the influence of the solvent used during the impregnation of fibres with PLA solution on the microstructure of the fibres despite the silica-calcium sol layer used.

The weakest conductivity of incubation fluids was recorded for the PAA composite. The most significant increase in conductivity occurred after the first hour of incubation; after that, these changes were no longer so rapid and occurred gradually to the end of the measurements. The results presented by M. Boguń [31] concerning research on alginate fibres showed that the process of degradation of calcium alginate fibres in a PCL (poly-ε-caprolactone) matrix composite began after about 2 weeks of incubation, which was manifested by an increase in the conductivity of DW. These changes with 10 wt.% of fibres in the composite did not exceed 8 μS/cm. However, for the tested PAA composite, the conductivity changes were much higher. The changes in the conductivity of DW up to 3 weeks are primarily associated with the release of BSA. This was also confirmed by EDS analysis, where sulphur and nitrogen associated with the protein were present for the initial PAA composite (FIG. 2b), but after 4 weeks of incubation these elements were not detected (FIG. 8b). The slight increase in conductivity in the following weeks is probably due to the degradation of alginate fibres. Partial degradation of the fibres is confirmed by changes in the composite microstructure. A difference in the arrangement of the fibres can be observed. The fibres clearly moved and swelled during incubation and partially covered the surface of the composite. The gel form probably facilitates their migration. The influence of the environment in which the material was incubated is clearly visible. After 4 weeks of incubation in PBS, as described above, it is difficult to identify alginate fibres, but the voids left by the fibres are visible (FIG. 3b).

Cell culture showed the proper morphology of cells in contact with the surface of the composites. Cells were spread on the surface and no apoptotic cells were observed (FIG. 9). However, the most intensive cell proliferation was visible in the case of PKA composite. This was confirmed by the results of NHOst cell viability presented in FIG. 10. In the case of PAA and PKA, a significant increase in cell number between 3 and 7 days of culture is visible. The significantly lower cell viability on the composites' surface compared to the control can be associated with their porous microstructure and cell proliferation into the composite, which made it difficult to precisely analyse their quantity.

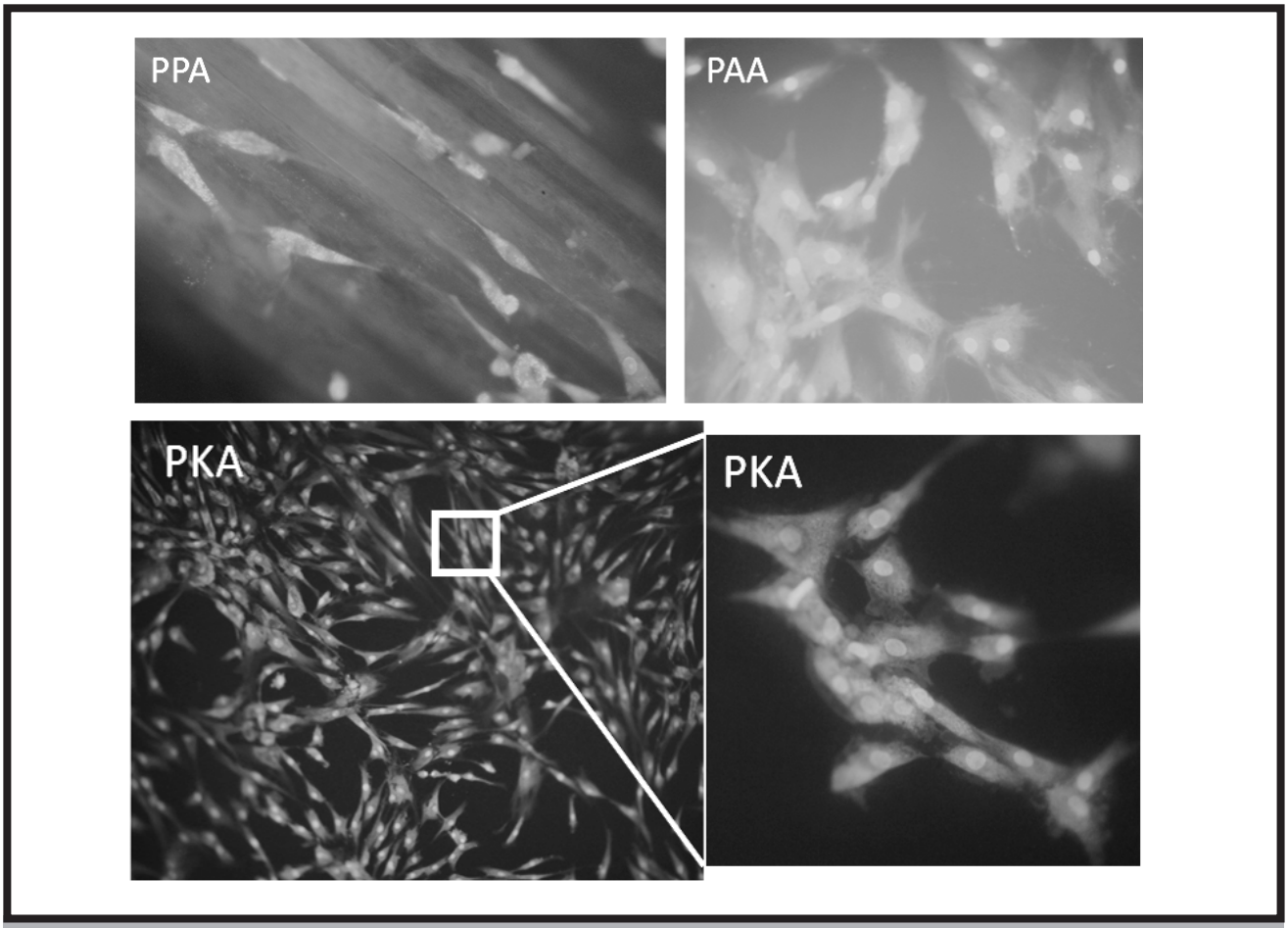

FIG. 9. Cell morphology on the composites' surface after 3 days of culture (PPA and PAA mag. 20x; PKA mag. 10x and 20x, respectively).

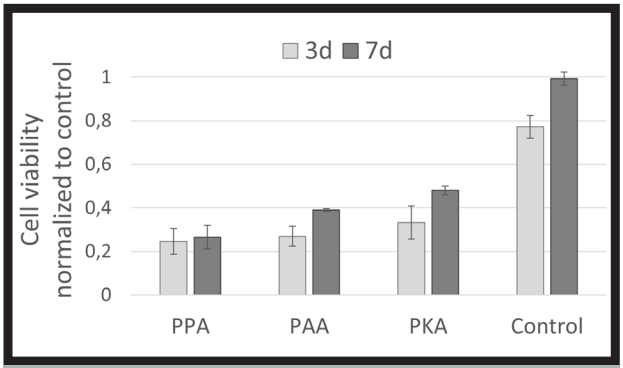

FIG. 10. NHOst cell viability determined by the CellTiter assay on days 3 and 7 of culture on the TCPS control surface and on the surfaces of the samples.

Conclusions

BSA was completely released from all tested composites during 3 weeks of incubation in PBS. The release process takes place from the first hours of incubation. Within the first day, this process is the fastest in the case of a composite with PLA fibres. This is related to only the surface adhesion of the protein on the fibres. In contrast to PLA fibres, the alginate fibres can absorb the BSA inside their volume thanks to high swelling ability in the water environment.

Studies have shown a clear difference between the forms of the alginate carrier, such as fibres or beads. The use of a fibrous form accelerates the release of protein, due to the increased number of interfaces, running along the entire length of the composite. They are fast diffusion routes allowing fluids to penetrate inside the composite and BSA to migrate outward. In the case of bead carriers, they are completely surrounded by a PLA matrix, and the interfaces do not come into contact with the environment.

In the developed composites, the degradation process begins with the carrier phases; the PLA matrix is characterized by greater stability.

All tested composites show bioactive potential connected with apatite precipitation during incubation in a simulated biological environment. The most intense growth of apatites with the optimal ratio of calcium to phosphorus can be observed for the PPA composite. This is most likely related to the presence of a silica-calcium sol stimulating the nucleation of calcium phosphates.

The cell viability test showed NHOst cell proliferation after 3 and 7 days of culture. The cells were characterized by the proper morphology. The cell viability assay indicates good biocompatibility of the tested composites.

The conception of the multifunctional role of the studied composites in potential application as bone scaffolds is summarized in FIG. 11, where the main 4 areas of their activity are presented.

Acknowledgements

This work was supported from the subsidy of the Ministry of Education and Science for the AGH University of Krakow (Project No 16.16.160.557).

Prof. Maciej Boguń (Lodz University of Technology, Department of Material and Commodity Sciences and Textile Metrology, Poland) for polylactide and alginate fibres manufacturing, Elżbieta Menaszek Ph.D. (Jagiellonian University, Medical College, Faculty of Pharmacy, Poland) for performing cell tests (including photos of cells) with a description of the research method and Agnieszka Daszyńska (AGH University of Krakow, Faculty of Materials Science and Ceramics, Department of Biomaterials and Composites, Poland) for help in data acquisition are gratefully acknowledged.

ORCID iD

A. Morawska-Chochół: https://orcid.org/0000-0003-0209-4402

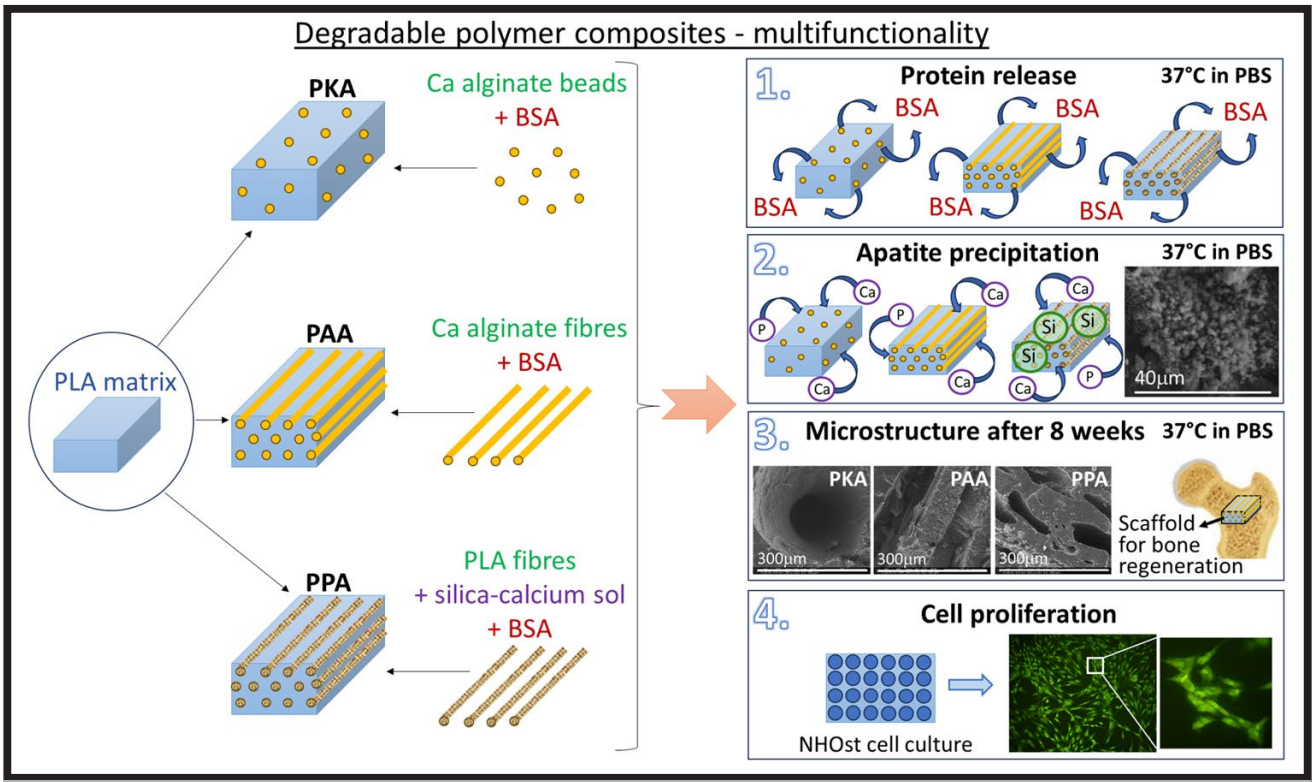

FIG. 11. Graphical summary of the results: scaffolds composition and the main areas of their activity.

References

[1] Dorogin J., Townsend J.M., Hettiaratchi M.H.: Biomaterials for protein delivery for complex tissue healing responses. Biomaterials Science 9 (2021) 2339-2361. http://doi.org/10.1039/d0bm01804j

[2] Echeverria Molina M.I., Malollari K.G., Komvopoulos K.: Design challenges in polymeric scaffolds for tissue engineering. Frontiers in Bioengineering and Biotechnology 9 (2021) 617141. http://doi.org/10.3389/fbioe.2021.617141

[3] Zhao D., Zhu T., Li J., Cui L., Zhang Z., Zhuang, X., Ding J.: Poly(lactic-co-glycolic acid)-based composite bone-substitute materials. Bioactive Materials 6 (2021) 346-360. http://doi.org/10.1016/j.bioactmat.2020.08.016

[4] Sheng Y., Gao J., Yin Z.Z., Kang J., Kong Y.: Dual-drug delivery system based on the hydrogels of alginate and sodium carboxymethyl cellulose for colorectal cancer treatment. Carbohydrate Polymers 269 (2021) 118325. http://doi.org/10.1016/j.carbpol.2021.118325

[5] Li H., Li P., Yang Z., Gao C., Fu L., Liao Z., Zhao T., et al.: Meniscal regenerative scaffolds based on biopolymers and polymers: Recent Status and Applications. Frontiers in Cell and Developmental Biology 9 (2021) 661802. http://doi.org/10.3389/fcell.2021.661802

[6] Pakulska M.M., Donaghue I.E., Obermeyer J.M., Tuladhar A., McLaughlin C.K., Shendruk T.N., Shoichet M.S.: Encapsulation-free controlled release: Electrostatic adsorption eliminates the need for protein encapsulation in PLGA nanoparticles. Science Advances 2 (2016) e1600519. http://doi.org/10.1126/sciadv.1600519

[7] Yao B., Ni C., Xiong C., Zhu C., Huang B.: Hydrophobic modification of sodium alginate and its application in drug controlled release. Bioprocess and Biosystems Engineering 33:4 33 (2009) 457-463. http://doi.org/10.1007/S00449-009-0349-2

[8] Lee B.K., Yun Y., Park K.: PLA micro- and nano-particles. Advanced Drug Delivery Reviews 107 (2016) 176. http://doi.org/10.1016/j.addr.2016.05.020

[9] Brzeziński M., Wedepohl S., Kost B., Calderón M.: Nanoparticles from supramolecular polylactides overcome drug resistance of cancer cells. European Polymer Journal 109 (2018) 117-123. http://doi.org/10.1016/J.EURPOLYMJ.2018.08.060

[10] Marincaș L., Farkas N.I., Barbu-Tudoran L., Barabás R., Toşa M.I.: Deep eutectic solvent PCL-based nanofibers as drug delivery system. Materials Chemistry and Physics 304 (2023) 127862. http://doi.org/10.1016/J.MATCHEMPHYS.2023.127862

[11] Li J., Ding J., Liu T., Liu J.F., Yan L., Chen X.: Poly(lactic acid) controlled drug delivery. In Industrial Applications of Poly(lactic acid). Advances in Polymer Science; Di Lorenzo, M., Androsch, R., Eds.; Springer: New York (2017); Vol. 282, pp. 109-138.

[12] Liu S., Qin S., He M., Zhou D., Qin Q., Wang H.: Current applications of poly(lactic acid) composites in tissue engineering and drug delivery. Composites Part B: Engineering 199 (2020) 108238. http://doi.org/10.1016/j.compositesb.2020.108238

[13] Sharma S., Gupta V., Mudgal D.: Experimental investigations on polydopamine coated poly lactic acid based biomaterial fabricated using 3D printing for orthopedic applications. Materials Chemistry and Physics 310 (2023) 128473. http://doi.org/10.1016/J.MATCHEMPHYS.2023.128473

[14] Pyza M., Brzezińska N., Kulińska K., Gabor J., Barylski A., Aniołek K., et al.: Polylactide-based composite materials for 3D printing and medical applications - the effect of basalt and silicon dioxide addition. Engineering of Biomaterials 166 (2022) 29-39. http://doi.org/10.34821/eng.biomat.166.2022.29-39

[15] Senatov F.S., Zadorozhnyy M.Y., Niaza K.V., Medvedev V.V., Kaloshkin S.D., Anisimova N.Y., Kiselevskiy M.V., Yang K.C.: Shape memory effect in 3D-printed scaffolds for self-fitting implants. European Polymer Journal 93 (2017) 222-231. http://doi.org/10.1016/J.EURPOLYMJ.2017.06.011

[16] Kumawat V.S., Bandyopadhyay-Ghosh S., Ghosh S.B.: Rationally designed biomimetic bone scaffolds with hierarchical porous-architecture: Microstructure and mechanical performance. Express Polymer Letters 17 (2023) 610-624. http://doi.org/10.3144/expresspolymlett.2023.45

[17] Gryń K.: Long-term mechanical testing of multifunctional composite fixation miniplates. Engineering of Biomaterials 157 (2020) 20-25. http://doi.org/10.34821/eng.biomat.157.2020.20-25

[18] Yadav P., Yadav B.: Preparation and characterization of BSA as a model protein loaded chitosan nanoparticles for the development of protein-/ peptide-based drug delivery system. Future Journal of Pharmaceutical Sciences 7 (2021) 200. http://doi.org/10.1186/s43094-021-00345-w

[19] Norudin N.S., Mohamed H.N., Yahya N.A.M.: Controlled released alginate-inulin hydrogel: Development and in-vitro characterization. AIP Conference Proceedings 2016 (2018) 20113. http://doi.org/10.1063/1.5055515

[20] Yang Z., Cui Y., Zhang Y., Liu P., Zhang Q., Zhang B.: Identification of imprinted sites by fluorescence detection method based on reversible dynamic bond modified template protein. Composites Part B: Engineering 223 (2021) 109154. http://doi.org/10.1016/j.compositesb.2021.109154

[21] Morawska-Chochół A.: Manufacturing of resorbable composite biomaterials containing protein. Materials and Manufacturing Processes 37 (2022) 782-791. http://doi.org/10.1080/10426914.2021.2001508

[22] Tang L., Chen Y.H., Wang Q., Wang X.H., Wu Q.X., Ding Z.F.: Microencapsulation of functional ovalbumin and bovine serum albumin with polylysine-alginate complex for sustained protein vehicle's development. Food Chemistry 368 (2022) 130902. http://doi.org/10.1016/j.foodchem.2021.130902

[23] Noble J.E.: Quantification of protein concentration using UV absorbance and Coomassie dyes. Methods in Enzymology 536 (2014) 17-26. http://doi.org/10.1016/B978-0-12-420070-8.00002-7

[24] Ilyas R.A., Sapuan S.M., Harussani M.M., Hakimi M.Y.A.Y., Haziq M.Z.M., Atikah M.S.N., Asyraf M.R.M., Ishak M.R., Razman M.R., Nurazzi N.M., Norrrahim M.N.F., Abral H., Asrofi M.: Polylactic acid (PLA) biocomposite: Processing, additive manufacturing and advanced applications. Polymers 13 (2021) 1326. http://doi.org/10.3390/polym13081326

[25] Amini M., Khavandi A.: Degradation of polymer-based composites in corrosive media: experimental attempts towards underlying mechanisms. Mechanics of Time-Dependent Materials 23 (2019) 153-172. http://doi.org/10.1007/S11043-018-09408-7

[26] Nochos A., Douroumis D., Bouropoulos N.: In vitro release of bovine serum albumin from alginate/HPMC hydrogel beads. Carbohydrate Polymers 74 (2008) 451-457. http://doi.org/10.1016/j.carbpol.2008.03.020

[27] Wells L.A., Sheardown H.: Extended release of high p*I* proteins from alginate microspheres via a novel encapsulation technique. European Journal of Pharmaceutics and Biopharmaceutics 65 (2007) 329-335. http://doi.org/10.1016/j.ejpb.2006.10.018

[28] Ko C.L., Wu H.Y., Lin Y.S., Yang C.H., Chen J.C., Chen W.C.: Modulating the release of proteins from aloaded carrier of alginate/gelatin porous spheres immersed in different solutions. Bio-Medical Materials and Engineering 28 (2017) 515-529. http://doi.org/10.3233/BME-171690

[29] Abifarin J.K., Obada D.O., Dauda E.T., Dodoo-Arhin D.: Experimental data on the characterization of hydroxyapatite synthesized from biowastes. Data in Brief 26 (2019) 104485. http://doi.org/10.1016/j.dib.2019.104485

[30] Chłopek J., Morawska-Chochół A., Szaraniec B.: The influence of the environment on the degradation of polylactides and their composites. Journal of Achievements in Materials and Manufacturing Engineering 43 (2010) 72-79. https://api.semanticscholar.org/CorpusID:137640086

[31] Boguń M., Krucińska I., Kommisarczyk A., Mikołajczyk T., Błażewicz M., Stodolak-Zych E., Menaszek E., Ścisłowska-Czarnecka A.: Fibrous polymeric composites based on alginate fibres and fibres made of poly-ε-caprolactone and dibutyryl chitin for use in regenerative medicine. Molecules 18 (2013) 3118-3136. http://doi.org/10.3390/molecules18033118

INVESTIGATION OF ANTIBACTERIAL PROPERTIES OF CERAMIC SUBSTRATES COATED WITH CALCIUM PHOSPHATE AND POLYMERIC NANOPARTICLES LOADED WITH ANTIBIOTICS

Anna Marszałek*, Iwona Pudełko-Prażuch, Małgorzata Krok-Borkowicz*

AGH University of Krakow,
Faculty of Materials Science and Ceramics,
Department of Biomaterials and Composites,
al. A. Mickiewicza 30, 30-059 Krakow, Poland
*e-mail: amarszalek@agh.edu.pl, krok@agh.edu.pl

Abstract

This study investigates a biomimetic method of deposition of bioactive calcium phosphate (CaP) layers on zirconium oxide substrates (ZrO_2). The substrates contained polymer nanoparticles of poly(L-lactide-co-glycolide) (PLGA) obtained using the double emulsion method with solvent evaporation. Three antibiotics were encapsulated within the nanoparticles: bacitracin, gentamicin sulphate, and hydrophobic gentamicin, prepared with the use of the ion pairing method. Nanoparticles were immobilized on the substrates using the drop casting or the co-deposition method. The microstructure of the layers and the distribution of the nanoparticles were assessed by scanning electron microscopy. The nanoparticles size and their zeta potential were measured using the dynamic light scattering method. The release of drugs over time was examined and the antibacterial properties were evaluated in contact with Staphylococcus aureus bacteria using the spectrophotometric method and the Kirby-Bauer test. The results show that the layer deposition method is effective and allows to obtain homogenous bioactive coatings. Nanoparticles were agglomerated on the surface or homogenously distributed in the CaP coating, depending on the process used to immobilize them. The drug release profile and antibacterial properties can also be modified by changing the process – the drop casting method allows to obtain a coating with a stronger antimicrobial effect and faster drug release.

Nanoparticles obtained by the double emulsion method with solvent evaporation have the required size to be immobilized between the CaP crystallites. Additionally, the encapsulation of drugs decreased the zeta potential of the nanoparticles, which was caused by the interaction of the drug and the polymer. Nanoparticles loaded with bacitracin showed weak antibacterial properties, as the growth inhibition zone in the Kirby-Bauer test was barely visible. Two other types of nanoparticles exhibited good antibacterial properties, exceptionally strong for those loaded with hydrophobic gentamicin.

[Engineering of Biomaterials 169 (2023) 11-17]

doi:10.34821/eng.biomat.169.2023.11-17

Submitted: 2023-07-16, Accepted: 2023-08-10, Published: 2023-08-14

Keywords: *ceramic substrates, polymer nanoparticles, poly(L-lactide-co-glycolide) (PLGA), hydrophobic gentamicin, biomimetic coating, calcium phosphate*

Introduction

With increasing life expectancy, diseases of the musculoskeletal system are becoming more frequent. They can be related to joint wear or be the result of complications after invasive orthopedic procedures [1]. In general, bone tissue has a natural ability to regenerate, but not all mechanical injuries or defects caused by diseases such as osteomyelitis, bone cancer, or osteoporosis can be spontaneously healed. In such cases, surgical intervention is required to fill the defect or replace the missing bone. Replacement can be made by bone grafting or by using a synthetic biomaterial, usually ceramic [1,2]. One of the diseases that is increasing in frequency is osteomyelitis, which often develops in the femur or spine. Untreated, it causes irreversible changes in the body, the need for amputation, and even death [3-5]. Osteomyelitis can be caused by many species of bacteria and fungi. *S. aureus* is responsible for the development of the disease in 80-90% of cases [6,7].

Zirconium dioxide is often used as a bone substitute to fill in gaps resulting from diseases or injuries [8,9]. ZrO_2 is an inert biomaterial, but it is possible to provide it with bioactive properties by coating it with another material, such as hydroxyapatite ceramics (HAp), which can bind to bone without creating fibrous tissue after implantation. The ZrO_2 substrate modified in this way allows cells to attach and proliferate on its surface [10]. One of the methods for obtaining such a coating is the biomimetic method, which mimics the first phase of integration of the material with bone tissue *in vivo*. It consists of precipitating calcium phosphate on the surface of the material immersed in simulated body fluid (SBF) and can be used to cover properly prepared metal, ceramic, polymer, or composite surfaces. The coatings obtained in this way have mechanical properties similar to those of natural bone and have high biocompatibility [11,12]. Changes in SBF concentration also allow to control roughness, which is important for the adhesion and proliferation of osteoblasts. The advantages of the method are the high homogeneity of the layers obtained and the possibility to coat devices characterized by various shapes and sizes, but it is necessary to control the process conditions: the temperature and pH of the solution [11-13].

In many applications, it is beneficial for implants to have antibacterial properties, as it reduces the risk of infection that could occur during the implantation process and prevents the adhesion of bacteria to the surface. Implants can also act as drug carriers, for example, by depositing nanoparticles loaded with antibiotics on their surface. Such a modification is valuable in the case of materials used to fill bone defects caused by surgical removal of infected tissue in osteomyelitis treatment [5,6].

The use of drug delivery systems (DDS) is more beneficial than containing the antibiotic itself in the coating. The main difficulty in the treatment of bone infections is the complexity of its tissue structure. The delivery of drugs to the bones, oral or intravenous, is often ineffective. Quite commonly, they are excreted from the body before they have a therapeutic effect at the target site, while the frequent administration of large doses of drugs can cause severe side effects [6]. Conventional antibiotic therapy guarantees that bacteria are eliminated from the whole body, but it has many disadvantages. Both the poor absorption of drugs from the digestive system and their rapid excretion from the body make it difficult to maintain a stable therapeutic level [14].

Meanwhile, DDS allows for a slower release, preventing a sudden increase in drug concentration to potentially toxic. Furthermore, for the same reason, drug levels are more stable over time. The drug can be released only in a specific place, thus avoiding systemic side effects. The behavior of the drug carrier can be modified to release substance only under certain conditions, e.g. local pH or temperature. In addition, prolonged release of the drug makes the absorption of the active substance easier, providing a better therapeutic effect. Targeted antibiotic therapy ensures better penetration of bone tissue by the drug, but attention must be paid to maintaining the appropriate concentration of the antibiotic, because microorganisms can acquire antibacterial resistance if it is not high enough [14,15].

Drug delivery systems are mostly based on nanoparticles (NPs). Particles with nanometric size easily penetrate infected bone tissue. The appropriate functionalization of their surface allows the therapeutic effect to be improved, for example, by providing an additional layer of molecules of another antibiotic or other compounds [6]. Polymer nanoparticles are stable colloidal structures in the form of nanocapsules or nanospheres differing in structure, size, and mechanism the drug is released. The manufacturing methods for both nanocapsules and nanospheres are well established [16,17].

This study investigates a biomimetic method of deposition of bioactive calcium phosphate (CaP) layers on zirconium oxide substrates (ZrO_2), containing polymer nanoparticles of poly(L-lactide-co-glycolide) (PLGA) obtained using the double emulsion method with solvent evaporation with three antibiotics encapsulated: bacitracin, gentamicin in the form of gentamicin sulphate and hydrophobic gentamicin, prepared with the use of the ion pairing method. Hydrophobic gentamicin was used in this study due to its higher encapsulation efficiency compared to basic gentamicin [18]. Similar research has already been conducted on the subject of CaP coatings with antibacterial NPs [1,19]. However, we compared different drugs and conducted thorough microbiological tests, which has not been done before.

Materials and Methods

Manufacturing nanoparticles

Drug-loaded NPs were prepared using the double emulsion method with solvent evaporation (FIG. 1). In the first step of NPs fabrication, 6 mg of each drug was added to 3 ml of a 2% solution of poly(L-lactide-*co*-glycolide) (PLGA, Polish Academy of Sciences, Zabrze, Poland) in dichloromethane (DCM, Chemland, Stargard, Poland) and mixed with ultrasounds for 3 min with an amplitude of 40% (Vibra Cell VCX130, Sonics, Newtown, CT, USA). The obtained solution was added to the 2% aqueous solution of poly(vinyl alcohol) (PVA, Sigma Aldrich, Steinheim, Germany) and mixed with ultrasounds for 3 min with an amplitude of 40% and then on a magnetic stirrer with a speed of 1000 rpm. After 24 h, the solutions were centrifuged for 20 min at a speed of 15 000 rpm (MPW-351R, MPW Med. instruments, Warszawa, Poland). 2 ml of supernatants were taken to investigate the encapsulation efficiency (EE) and drug loading (DL). The remaining volume was removed.

Then 20 ml of ultra-high quality water was added and the particles were centrifuged again. This process was repeated 3 times. After removing the water from the last centrifugation, 3 ml of ultra-high quality water was added and the obtained sample was placed at a temperature of −80ºC for 24 h. The last step in the preparation of particles was the freeze-drying process, which was carried out for 24 h (Christ Alpha 1–2 LDplus, Martin Christ, Osterode am Harz, Germany). To prepare empty NPs, mixing antibiotics with PLGA in the first step was omitted, and PLGA was sonicated alone to keep the same conditions, the rest of the process was conducted without any changes. The drugs used were bacitracin (Sigma Aldrich, Steinheim, Germany), gentamicin sulphate (Sigma Aldrich, Steinheim, Germany), and hydrophobic gentamicin (GEN AOT), obtained as described in [18]. Briefly, gentamicin sulphate was modified into a hydrophobic complex, by hydrophobic ion pairing of gentamicin with the anionic surfactant dioctyl sulfosuccinate sodium salt (AOT, Sigma-Aldrich, Germany).

Nanoparticles characterization

The size and zeta potential of NPs were measured using the dynamic light scattering method (DLS, Zetasizer nano-ZS, Malvern, UK). Three measurements were made for each type of particles. The encapsulation efficiency and drug loading were investigated using supernatants collected after the first centrifugation of NPs. To quantify the amount of drug in them, an o-phtaldialdehyde (OPA, Sigma-Aldrich, Germany) assay was conducted. This test is based on the reaction of OPA with the drug present in the supernatant and the fluorescence measurement. The OPA reagent was prepared by mixing o-phtaldialdehyde with methanol, 2-mercaptoethanol, and borate buffer. Then 50 µl of supernatant (three samples for each) was transferred to a black 96-well plate and 50 µl of OPA reagent was added to each. Based on the results of fluorescence measurement, EE and DL were calculated according to formulas (1) and (2), respectively:

$$EE = \frac{\text{mass of used drug - mass of drug in supernatant}}{\text{mass of used drug}} \cdot 100\ [\%] \quad (1)$$

$$DL = \frac{\text{mass of used drug - mass of drug in supernatant}}{\text{mass of obtained NPs}} \cdot 100\ [\%] \quad (2)$$

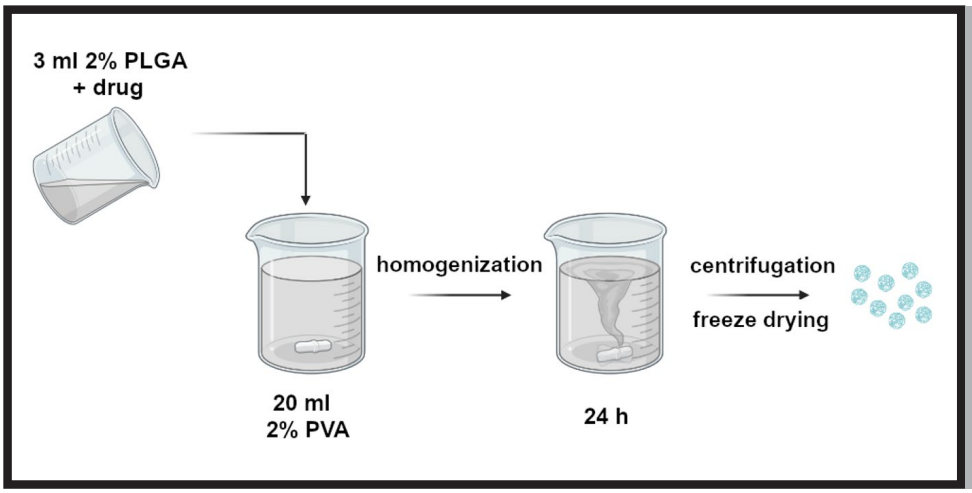

FIG. 1. Schematic process of NPs manufacturing.

Coating deposition

Round zirconium oxide substrates 0.8 cm in diameter, each obtained by pressing and sintering 1.3 g of zirconium oxide powder, were used. After sintering, they were polished and treated with phosphoric acid to create functional Zr-OH groups, which effectively participate in the process of apatite formation in the body's environment [20].

Bioactive coatings on the surface of the substrates were obtained using the biomimetic method based on the precipitation of CaP crystals from the simulated body fluid (SBF) solution. To coat the substrates with a CaP layer, a two-step precipitation method with the use of solutions similar to concentrated SBF was applied. The first step solution was prepared as detailed by Costa *et al.* [12], while the second one as described in [11] (FIG. 2).

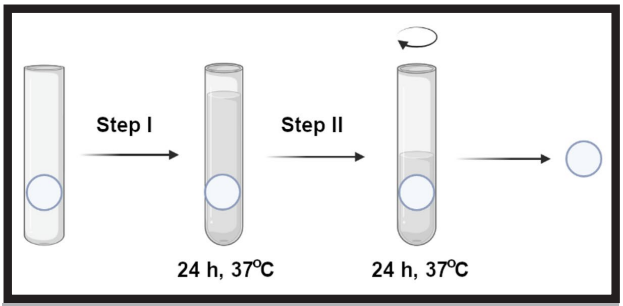

FIG. 2. Schematic representation of the deposition process of calcium phosphate.

Immobilization of nanoparticles

NPs were incorporated into the CaP layers using two methods:

• Co-deposition method

In this method, the dispersion of NPs (10 mg/ml) was added to the solution used during step II of the deposition process.

• Drop casting method

After the second step of the layer deposition process was completed, 100 µl of NPs dispersed in water at a concentration of 2 mg/ml was applied to the substrate surface and left to dry at room temperature.

Layers morphology

Pictures of layers without NPs after steps I and II of different depositions and layers with NPs immobilized by the co-deposition and the drop casting method were taken using a scanning electron microscope (SEM, GeminiSEM 500, Zeiss, Germany).

Drug release profile

To determine drug release profiles, substrates with NPs were closed in dialysis bags (ZelluTrans, Roth, Germany, cut-off 12-14 kDa) and placed in vials filled with 20 ml of PBS. The experiment was carried out at 37°C for 30 days. In predetermined periods of time, 2 ml of PBS was collected and replaced with the same amount of fresh PBS solution. The amount of drug in the collected solution was then quantified using the OPA assay.

Antimicrobial effect

To verify the antibacterial properties of the obtained coatings, the tests with *S. aureus* (ATCC MSSA 25923) were performed. Bacteria cultures were passaged twice before analysis by sieving onto slants with nutrient agar and incubated for 24 h at 37°C ± 1°C. Scaffolds containing empty or loaded NPs samples were incubated in 2 ml of PBS for 24 h at 37°C to obtain the extracts.

Kirby-Bauer test

A well was cut in the agar in which 100 µl of a 500 mg/ml suspension of particles was placed. After 24 h, photos were taken and growth inhibition zones were measured.

Spectrophotometric method

Extracts were prepared by placing coated substrates with empty NPs and NPs loaded with bacitracin, gentamicin, or hydrophobic gentamicin in 2 ml of PBS. The bacteria were suspended in a sterile solution of nutrient broth and buffered saline in a 1:3 ratio to obtain a bacterial count of ~10^6 cell forming units (CFU)/ml. The inoculum was then added to the test tubes containing the extracts of the test samples in a 1:1 ratio. A control sample containing a bacterial solution without the addition of any extract was also prepared. Tubes containing inoculated test materials and control materials were incubated at 36°C ± 0.1°C for 24 h. The microbial viability was assessed using the spectrophotometric method (UV Vis Shimadzu, Japan) by measuring the optical density of the prepared solutions at a wavelength of 600 nm. Test samples were taken from the incubated solutions at defined time intervals.

Statistical analysis of the results was performed using a one-way analysis of variance (one-way ANOVA).

Results and Discussions

Characterization of nanoparticles

TABLE 1 shows the results of the measurements of the zeta potential and nanoparticles size using the DLS method. The size range of the particles and the average size are included. For each type of NPs with drugs, the average size is smaller than that of empty NPs, with the smallest being those with gentamicin. The size of NPs containing gentamicin and those with AOT-modified gentamicin is in the same range, but their average size is significantly different – for NPs with AOT-modified gentamicin it is larger by about 40 nm. The difference between all NPs is statistically significant, which means that they do not belong to the same population. This phenomenon was also observed in [19] for gentamicin and bacitracin loaded NPs and in [21], where encapsulation of gentamicin in PLGA NPs caused a decrease in particle size.

TABLE 1. Size range (n = 3) and average size of the NPs, zeta potential (n = 3), encapsulation efficiency (EE), and drug loading (DL) of respective NPs.

	Size range [nm]	Average size [nm] ± SD	Zeta potential [mV] ± SD	EE [%] ± SD	DL [%] ± SD
Empty NPs	142-396	314 ± 7	-10.3 ± 0.7	-	-
GEN NPs	122-459	241 ± 4	-12.3 ± 0.4	38.7 ± 9.9	3.5 ± 0.9
BAC NPs	122-615	271 ± 2	-15.1 ± 0.4	56.9 ± 2.4	5.2 ± 0.2
GEN AOT NPs	122-459	278 ± 2	-11.1 ± 0.5	99.9 ± 0.1	9.2 ± 0.2

The zeta potential decreased for all types of NPs with drugs, which is caused by the interaction of the drug and polymer. The lowest zeta potential was measured for nanoparticles with bacitracin. Moreover, the zeta potential of NPs loaded with hydrophobic gentamicin was higher than that for non-modified gentamicin with a statistically significant difference. However, many studies showed the opposite trend [1,18,19,21,22], suggesting that other external factors influence the properties of NPs, which requires further research.

The results of the calculations of EE and DL are also presented in TABLE 1. For NPs with bacitracin, a higher efficiency of encapsulation and drug loading was achieved than for particles with gentamicin, while the best encapsulation was achieved in the case of NPs with hydrophobic gentamicin, which proves the effectiveness of this modification, also described in other studies, such as [1,18] or [23], where nearly 100% EE was reported.

Coatings morphology

FIG. 3 shows photos of the obtained CaP layers without the addition of NPs, after the first and after the second step of deposition, respectively. As seen in FIGs 3 A and B, the layer after the first step is inhomogeneous and areas not covered with CaP crystals are visible, as the purpose of the first step is to deposit CaP nuclei. Because of that, a two-step process is necessary, as FIGs 3 C and D show a homogeneous coating with well-formed CaP crystals. The finished coatings look very similar to those reported in papers [12,19], where the authors used the same precipitation method.

FIG. 4 shows the microstructure of the coatings with NPs, after co-deposition and after application of the drop casting method. Few particles are visible on the surface of the layer produced by the co-deposition process, while after the drop casting method many particles forming clusters can be seen. During co-deposition, the nanoparticle suspension was added to the solution, so the particles can also occur under the CaP crystals. If a drop of the suspension is placed on the surface, the particles do not penetrate the CaP layer and more of them are visible. However, there are fewer particles visible after the use of the co-deposition method; they seem to be more homogenously distributed between the CaP crystals as compared to NPs immobilized with the drop casting method, which are highly agglomerated. Similar results can be seen in [19], where exactly the same method of NPs immobilization was used.

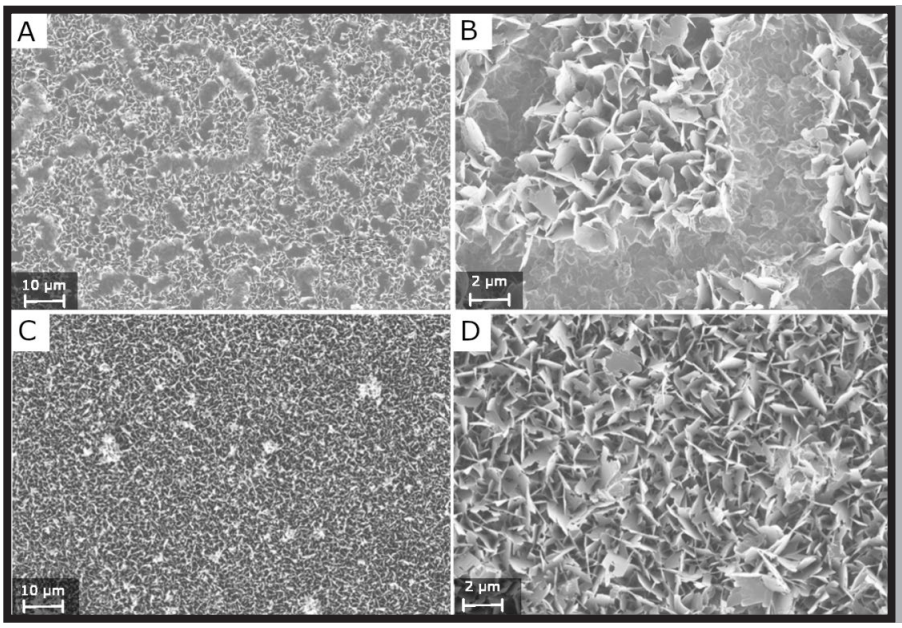

FIG. 3. SEM images of CaP coating morphology after the first (A, B) and second step (C, D) of the deposition process.

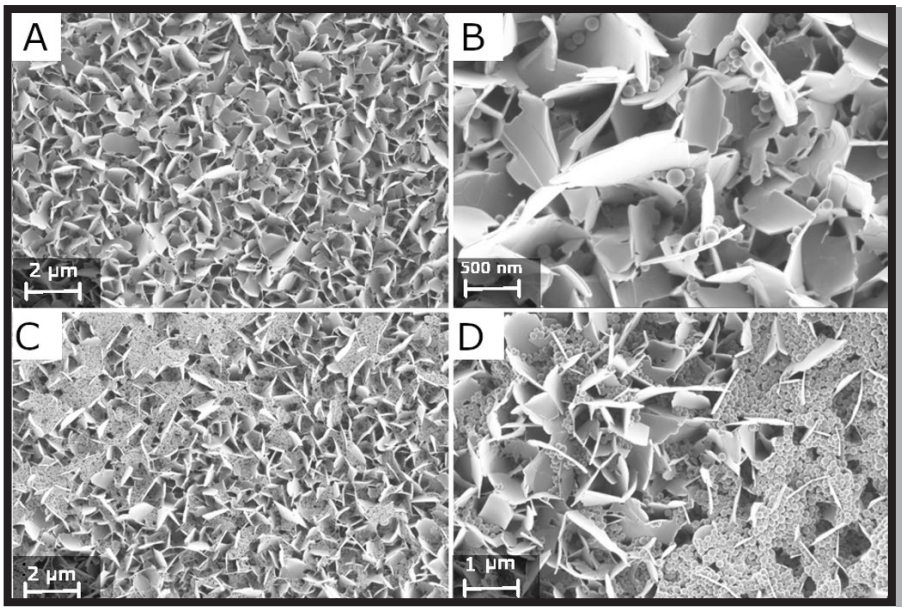

FIG. 4. SEM images of CaP coating with NPs immobilized with co-deposition (A, B) and drop casting method (C, D).

Drug release profile

FIG. 5 shows the release of drugs from the manufactured ZrO_2 samples surface-modified with CaP with drug-loaded NPs. For each sample, a much higher drug concentration was achieved for the particles deposited using the drop casting method, due to the greater number of particles on the surface of the layer, as shown by the SEM studies (FIG. 4). At the end of the study, it was found that the lowest concentration was achieved with gentamicin and the highest with bacitracin.

For both NPs loaded with GEN and GEN AOT in the beginning, the drug was released in a similar manner. However, the final concentration of hydrophobic gentamicin was higher than that of gentamicin sulphate, which may be due to better encapsulation efficiency of this drug: almost 100% of the GEN AOT was encapsulated in NPs (TABLE 1). A similar drug release profile was obtained in the paper [1] for NPs loaded with GEN and GEN AOT, the latter being released faster and reaching a higher concentration at the end of the study. Also in [22], where PLGA NPs loaded with gentamicin were studied, after a burst release, the drug was slowly released until the end.

Antimicrobial properties

FIG. 6 shows the growth inhibition zones of *S. aureus* bacteria in contact with suspended NPs according to the Kirby-Bauer test. As expected, the presence of empty NPs did not affect bacterial growth. Bacitracin NPs had a weak effect, so they were not included in further antibacterial studies. Although more drug was released from the nanoparticles containing bacitracin (FIG. 5), the larger inhibition zone of bacterial growth was obtained for both gentamicin and AOT-modified gentamicin, suggesting that those two antibiotics are more effective against this particular strain of bacteria. Moreover, studies report that bacitracin generally has a weaker antibacterial effect on *S. aureus* than gentamicin [24].

Both particles with gentamicin and AOT-modified gentamicin showed good antibacterial activity, with the growth inhibition zone for hydrophobic gentamicin being larger, indicating a stronger antibacterial effect. The same trend was observed in other studies [18,25], proving that the ion pairing of gentamicin with AOT does not affect the potency of the antibiotic in a negative way.

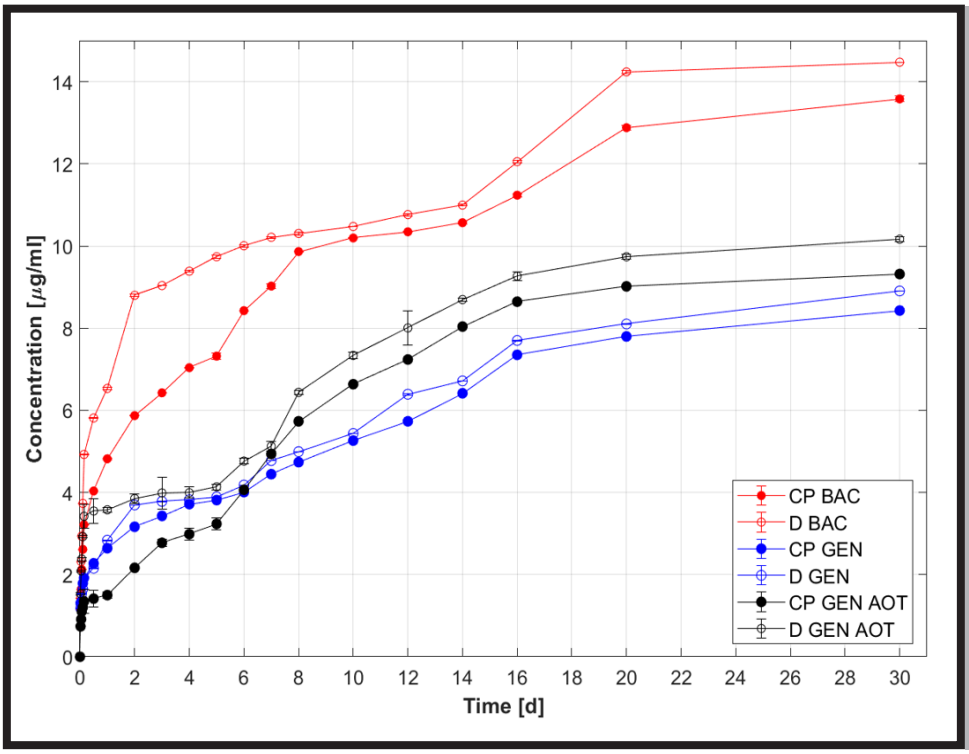

FIG. 5. Drug release profile for all types of substrates prepared using the co-deposition (CP) or drop casting (D) method with particles loaded with bacitracin, gentamicin, and hydrophobic gentamicin (n = 3).

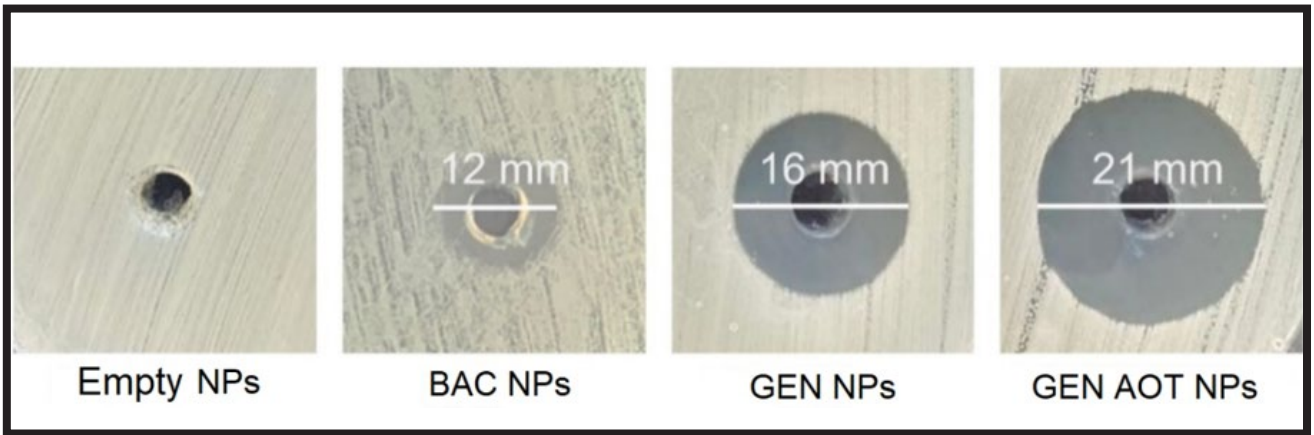

FIG. 6. Growth inhibition zones of *S. aureus* bacteria in contact with different types of NPs (n = 3).

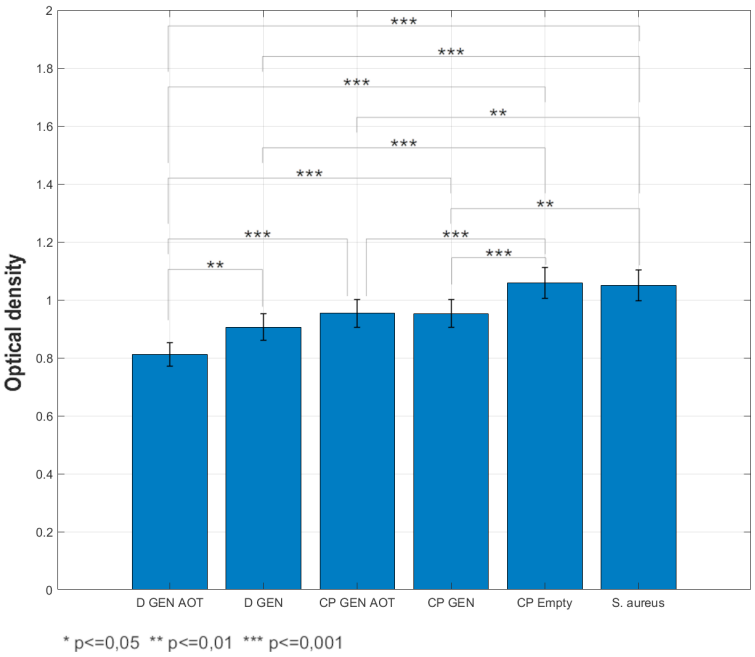

FIG. 7. Optical density for *S. aureus* and *S. aureus* in contact with extracts of samples coated with CaP layer that contains different types of antibiotic-loaded NPs (n = 3).

Spectrophotometric method

FIG. 7 presents the results of the optical density measurement of extracts at different time points, which represents the growth of bacteria. The highest optical density, and thus the weakest antibacterial properties, showed extracts from substrates with empty NPs, as expected. This confirms the result of the Kirby-Bauer test. In the case of NPs with non-modified gentamicin and AOT-modified gentamicin, inhibition of bacterial growth can be observed.

Regardless of the drug used, extracts from samples coated using the co-deposition method have weaker antibacterial properties due to slower drug release (FIG. 5). It is caused by a more homogenous distribution of NPs in the coating – in the case of the drop casting method, the majority are located on the surface, where release is easier (compare FIGs 4 A, B and C, D).

Conclusions

The aim of this study was to obtain a CaP coating on ceramic substrates and immobilize PLGA nanoparticles with antibacterial drugs encapsulated: bacitracin, gentamicin, and AOT-modified hydrophobic gentamicin. Their size and zeta potential were characterized, as well as the drug loading and encapsulation efficiency. The release of drugs from the coatings on the ZrO_2 substrates and antibacterial properties were also investigated.

The biomimetic method of depositing bioactive layers on ZrO_2 substrates and incorporating the prepared NPs by two methods: co-deposition and drop casting proved to be effective. SEM pictures show homogenous coating and the presence of the NPs. Particles produced using the double emulsion method have the required nanometric size. Loading them with any of the three tested drugs caused a reduction in both the size and zeta potential due to the interaction between PLGA and antibiotics, with GEN NPs being the smallest and GEN AOT the largest.

The conversion of gentamicin sulphate into hydrophobic gentamicin by ion pairing was found to be an effective way to fabricate particles with significantly improved encapsulation efficiency and drug loading values. NPs with hydrophobic gentamicin coupled with AOT are characterized by a highly improved encapsulation efficiency of 99.9 ± 0.1%.

Although both methods of immobilizing NPs were effective, the release of the drug was faster when the drop casting method was used. This is because NPs agglomerate on the surface of the substrate in greater quantity, while in the co-deposition method they are also present below the surface of the deposited layers. Because of this, the method of deposition allows to control the rate and profile of drug release. Antibacterial tests of the obtained materials showed that both particles containing gentamicin sulphate and gentamicin modified with AOT exhibit antibacterial properties, inhibiting the growth of *S. aureus* bacteria. Bacitracin showed weak antimicrobial activity in the Kirby-Bauer test, and thus was not tested with the spectrophotometric method.

In summary, the response of bacteria in contact with either produced NPs or extracts from the substrates depends on the type of drug – GEN AOT being the most efficient. The method used to immobilize nanoparticles directly translates into antibacterial activity of the substrate. By changing manufacturing conditions of NPs and coatings, the antibacterial activity of samples can be adjusted to the desired application.

Acknowledgements

This research was funded by the subsidy (No 16.16. 160.557) for the AGH University of Krakow and the Polish National Agency for Academic Exchange (NAWA, PPN/ BDE/2021/1/00021).

The authors also thank Roksana Kurpanik from the Department of Biomaterials and Composites, Faculty of Materials Science and Ceramics, AGH University of Krakow, for her assistance in investigating and discussing the antimicrobial properties of coatings and nanoparticles.

ORCID iD

A. Marszałek: https://orcid.org/0009-0005-2511-2070
I. Pudełko-Prażuch: https://orcid.org/0000-0002-1024-9374
M. Krok-Borkowicz: https://orcid.org/0000-0002-9415-0282

References

[1] Pudełko I., Moskwik A., Kwiecień K., Kriegseis S., Krok-Borkowicz M., Schickle K., Ochońska D., Dobrzyński P., Brzychczy-Włoch M., Gonzales-Julian J., Pamuła E.: Porous zirconia scaffolds functionalized with calcium phosphate layers and PLGA nanoparticles loaded with hydrophobic gentamicin. International Journal of Molecular Sciences 24(9) (2023) 8400.

[2] Glauser R., Schupbach P.: Early bone formation around immediately placed two-piece tissue-level zirconia implants with a modified surface: an experimental study in the miniature pig mandible. International Journal of Implant Dentistry 8(1) (2022) 37.

[3] Nair R., Schweizer M.L., Singh N.: Septic arthritis and prosthetic joint infections in older adults. Infectious Disease Clinics of North America 31(4) (2017) 715-729.

[4] Alder K.D., Lee I., Munger A.M., Kwon H.-K., Morris M.T., Cahill S.V., Back J., Yu K.E., Lee F.Y.: Intracellular Staphylococcus aureus in bone and joint infections: a mechanism of disease recurrence, inflammation, and bone and cartilage destruction. Bone 141 (2020) 115568.

[5] Pontes A.P., Welting T.J.M., Rip J., Creemers L.B.: Polymeric nanoparticles for drug delivery in osteoarthritis. Pharmaceutics 14(12) (2022) 2639.

[6] Aguilera-Correa J.J., Gisbert-Garzarán M., Mediero A., Fernández-Aceñero M.J., de-Pablo-Velasco D., Lozano D., Esteban J., Vallet-Regí M.: Antibiotic delivery from bone-targeted mesoporous silica nanoparticles for the treatment of osteomyelitis caused by methicillin-resistant Staphylococcus aureus. Acta Biomaterialia 154 (2022) 608-625.

[7] Jiang T., Yu X., Carbone E.J., Nelson C., Kan H.M., Lo K. W.-H.: Poly aspartic acid peptide-linked PLGA based nanoscale particles: potential for bone-targeting drug delivery applications. International Journal of Pharmaceutics 475 (2014) 547-557.

[8] Thu M.K., Kang Y.S., Kwak J.M., Jo Y.-H., Han J.-S., Yeo I.-S.L.: Comparison between bone–implant interfaces of microtopographically modified zirconia and titanium implant. Scientific Reports 13(1) (2023) 11142.

[9] Zhao Y., Li P., Dong P., Zeng Y., Chen J.: Investigation on 3D printing ZrO2 implant abutment and its fatigue performance simulation. Ceramics International 47(1) (2021) 1053-1062.

[10] Idaszek J., Jaroszewicz J., Choińska E., Górecka Z., Hyc A., Osiecka-Iwan A., Wieluńska-Kuś B., Święszkowski W., Moskalewski S.: Toward osteomimetic formation of calcium phosphate coatings with carbonated hydroxyapatite. Biomaterials Advances 149 (2023) 213403.

[11] Tas A.C., Bhaduri S.B.: Rapid coating of Ti6Al4V at room temperature with a calcium phosphate solution similar to 10× simulated body fluid. Journal of Materials Research 19(9) (2004) 2742-2749.

[12] Costa D.O., Allo B.A., Klassen R., Hutter J.L., Dixon S.J., Rizkalla A.S.: Control of surface topography in biomimetic calcium phosphate coatings. Langmuir 28(8) (2012) 3871-3880.

[13] Dziadek M., Zagrajczuk B., Menaszek E., Cholewa-Kowalska K.: A new insight into in vitro behaviour of poly(ε-caprolactone)/bioactive glass composites in biologically related fluids. Journal of Materials Science 53(6) (2018) 3939-3958.

[14] Nandi S.K., Bandyopadhyay S., Das P., Samanta I., Mukherjee P., Roy S., Kundu B.: Understanding osteomyelitis and its treatment through local drug delivery system. Biotechnology Advances 34(8) (2016) 1305-1317.

[15] Wang Y., Yuan Q., Feng W., Pu W., Ding J., Zhang H., Li X., Yang B., Dai Q., Cheng L., Wang J., Sun F., Zhang D.: Targeted delivery of antibiotics to the infected pulmonary tissues using ROS-responsive nanoparticles. Journal of Nanobiotechnology 17(1) (2019) 103.

[16] Sur S., Rathore A., Dave V., Reddy K.R., Chouhan R.S., Sadhu V.: Recent developments in functionalized polymer nanoparticles for efficient drug delivery system. Nano-Structures & Nano-Objects 20 (2019) 100397.

[17] Deirram N., Zhang C., Kermaniyan S.S., Johnston A.P.R., Such G.K.: pH-Responsive polymer nanoparticles for drug delivery. Macromolecular Rapid Communications 40(10) (2019) 1800917.

[18] Kwiecień K., Pudełko I., Knap K., Reczyńska-Kolman K., Krok-Borkowicz M., Ochońska D., Brzychczy-Włoch M., Pamuła E.: Insight in superiority of the hydrophobized gentamycin in terms of antibiotics delivery to bone tissue. International Journal of Molecular Sciences 23(20) (2022) 12077.

[19] Pudełko I., Desante G., Pamuła E., Schickle K., Krok-Borkowicz M.: The encapsulation of antibacterial drugs in polymer nanoparticles and their use in drug delivery systems on ZrO_2 scaffold with bioactive coating. Engineering of Biomaterials 161 (2021) 21-27.

[20] Uchida M., Kim H.-M., Kokubo T., Nawa M., Asano T., Tanaka K., Nakamura T.: Apatite-forming ability of a zirconia/alumina nanocomposite induced by chemical treatment. Journal of Biomedical Materials Research 60(2) (2002) 277-282.

[21] Ciocilteu M.-V., Nicolaescu O. E., Mocanu A. G., Nicolicescu C., Rau G., Neamtu J., Amzoiu E., Amzoiu E., Oancea C., Turcu-Stiolica A.: Process optimization using quality by design (QBD) approach of a gentamicin loaded PLGA biocomposite. Journal of Science and Arts 21(4) (2021) 1069-1080.

[22] Posadowska U., Brzychczy-Włoch M., Pamuła E.: Gentamicin loaded PLGA nanoparticles as local drug delivery system for the osteomyelitis treatment. Acta of Bioengineering and Biomechanics 17(3) (2015).

[23] Imbuluzqueta E., Gamazo C., Lana H., Campanero M.- Á., Salas D., Gil A.G., Elizondo E., Ventosa N., Veciana J., Blanco--Prieto M.J.: Hydrophobic Gentamicin-Loaded Nanoparticles are Effective against Brucella melitensis Infection in Mice. Antimicrobial Agents and Chemotherapy 57(7) (2013) 3326-3333.

[24] Dadpour S., Hosseini Doust R.: Synergistic Effects of Gold Nanoparticles Mixed with Gentamicin, Erythromycin, Clindamycin, Bacitracin, and Polymyxin B against Staphylococcus aureus, Staphylococcus saprophyticus, Staphylococcus epidermidis, Enterococcus faecium and Enterococcus faecalis. Iranian Journal of Medicinal Microbiology 16(4) (2022) 324-335.

[25] Ter Boo G.A., Grijpma D.W., Richards R.G., Moriarty T.F., Eglin D.: Preparation of gentamicin dioctyl sulfosuccinate loaded poly(trimethylene carbonate) matrices intended for the treatment of orthopaedic infections. Clinical Hemorheology and Microcirculation 60(1) (2015) 89-98.

POLY(L-LACTIDE-CO-GLYCOLIDE) MICROPARTICLES EMULSIFIED BY MIXING AND IN A MICROFLUIDIC DEVICE FOR POTENTIAL BOTTOM-UP BONE TISSUE ENGINEERING

Stanisław Marecik*, Małgorzata Krok-Borkowicz, Elżbieta Pamuła

AGH University of Krakow,
Faculty of Materials Science and Ceramics,
Department of Biomaterials and Composites,
al. A. Mickiewicza 30, 30-059 Krakow, Poland
*e-mail: smarecik@agh.edu.pl

Abstract

The aim of this study was to obtain degradable poly(L-lactide-co-glycolide) (PLGA) microparticles (MPs) with a controlled size for bottom-up bone tissue engineering. The particles were produced using the classical single water/oil emulsification method by mixing with a magnetic stirrer and by using a novel approach based on the application of a microfluidic device. This study involved a thorough investigation of different concentrations of PLGA and poly(vinyl alcohol) (PVA) during microparticle fabrication. The oil phase was PLGA dissolved in dichloromethane or ethyl acetate at 1%, 2% and 4% w/v concentrations. The water phase was an aqueous solution of PVA at concentrations of 0.5%, 1%, 2%, 2.5%, 4% and 5% w/v. The size and size distribution of the MPs were evaluated with an optical microscope. Obtained MPs were incubated in contact with osteoblast-like MG-63 cells and after days 1 and 3, the cell viability was evaluated using the reduction of resazurin and the fluorescence live/dead staining. The results showed that for each concentration of PVA, the size of the MPs increased with an increase in the concentration of PLGA in the oil phase. The MPs obtained with the use of the microfluidic device were characterized by a smaller size and lower polydispersity compared to those obtained with emulsification by mixing. Both methods resulted in the generation of MPs cytocompatible with MG-63 cells, what paves the way to consider them as scaffolds for bottom-up tissue engineering.

Keywords: *microparticles, poly(L-lactide-co-glycolide) (PLGA), water/oil emulsification, microfluidic device, bottom-up tissue engineering*

Introduction

Bone tissue engineering is promising in the treatment of bone tissue defects resulting from trauma, infections, or tumour resection [1]. Tissue engineering is based on two approaches, the first being the traditional top-down approach, using well-defined porous scaffolds supplemented with growth factors on which cells are deposited, cultured, and finally expected to form bone tissue. All these phenomena are correlated with the degradation of the scaffold material [2]. However, this classical approach has some limitations, such as difficulties in cell penetration to the central part of the scaffold, poor nutrients diffusion, and lack of proper vascularization [3]. A different strategy that solves these problems is the bottom-up approach, which is based on the creation of larger tissue structures by the assembly of microscaffold-cell constructs [4]. These microscaffolds can have a form of degradable microparticles on which cells can be deposited and cultured in static or dynamic conditions, thus assuring better diffusion of nutrients and waste removal. Furthermore, these microparticles can be loaded with drugs with a defined release time or with biologically active particles such as hydroxyapatite to ensure better osseointegration [5].

The material that demonstrates very good performance in bone regeneration is poly(L-lactide-co-glycolide) (PLGA), which is a biocompatible and biodegradable linear polyester [6]. It is possible to control its degradation time through the lactide to glycolide ratio in the polymer composition [7]. PLGA has many advantages, such as easy control of size, shape, and physical properties, which make it attractive for use in bone tissue engineering.

The results obtained in our group on PLGA microparticles show that they support adhesion, growth, and osteogenic differentiation of mesenchymal stem cells and can form microparticle/cell/extracellular matrix constructs suitable for bottom-up tissue engineering [8].

PLGA microparticles can be obtained by various techniques. One of them is a batch water/oil (W/O) emulsification method by mixing [9]. This is a method that allows to produce microparticles, but with high polydispersity. To achieve better homogeneity of the resulting samples, a microfluidic device can be used to produce microparticles [10]. Microfluidic devices operate on the basis of a co-flow of two immiscible phases [11] and produce microparticles by squeezing of the dispersed phase by the water phase. We hypothesize that the use of microfluidic device, due to better control of flow parameters, is expected to enhance the uniformity of PLGA microparticles, providing a platform that holds promise for improved cytocompatibility in bottom-up bone tissue engineering.

The aim of the study was: (1) to optimize the parameters of PLGA MPs manufacturing by a single water/oil emulsification method by mixing to produce microparticles with the lowest polydispersity, that can be achieved with this approach; (2) to use these conditions in the microfluidic device to generate MPs presumably with even lower polydispersity; and (3) to test the cytocompatibility of the obtained microparticles with MG-63 osteoblast-like cells.

[Engineering of Biomaterials 169 (2023) 18-22]

doi:10.34821/eng.biomat.169.2023.18-22

Submitted: 2023-07-20, Accepted: 2023-08-16, Published: 2023-08-18

Materials and Methods

Preparation of PLGA microparticles

The microparticles (MPs) were obtained by two techniques: single emulsification by mixing with a magnetic stirrer and a microfluidic device (RayDrop, Fluigent). In the case of emulsification by mixing (FIG. 1), to prepare the oil phase, PLGA (85:15, M_n = 100, M_w/M_n = 2.0, Center of Polymer and Carbon Materials of the Polish Academy of Sciences, Zabrze, Poland) was dissolved in dichloromethane (DCM, POCH Basic) at concentrations of 1%, 2% and 4% w/v. As the water phase, 0.5%, 1%, 2%, 2.5% and 4% w/v aqueous solutions of poly(vinyl alcohol) (PVA, Mowiol 4-88, Sigma-Aldrich) were prepared. PLGA solutions were added to a water phase while mixing at a speed of 800 rpm on a magnetic stirrer (MS-52M, Jeio Tech) at room temperature. The emulsions were then stirred for 24 h to evaporate the solvent. After this time, the MPs were drained under vacuum and dried in an incubator at 37°C for 24 h.

In the second production technique, using a microfluid device (RayDrop, Fluigent, FIG. 2A), the oil phase was PLGA dissolved in ethyl acetate (EA, POCH Basic) at a concentration of 2% w/v. As a water phase, an aqueous solution of PVA at a concentration of 2% w/v was prepared. First, the flow rate in the jetting regime (FIG. 2B) was determined by setting the flow rate to 100 µl/min and for the dispersed phase to 20 µl/min. Then the flow velocities of both phases were simultaneously reduced to 10 µl/min for the continuous phase and 0.6 µl/min for the dispersed phase. As a result, the flow in the dripping regime (FIG. 2C) was obtained, thus producing microparticles. The microparticles then fell into a 2% w/v PVA solution in water, which was stirred at a speed of 800 rpm on a magnetic stirrer. After the process was completed, the particles were stirred for another 24 h to evaporate the EA. Then they were drained under vacuum and dried in an incubator for 24 h at 37°C.

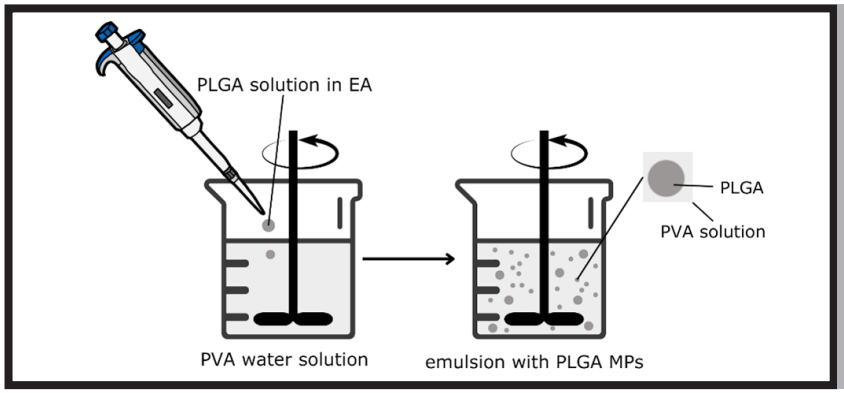

FIG. 1. Scheme of single emulsification method by mixing with a magnetic stirrer.
EA – ethyl acetate
PLGA – poly(L-lactide-co-glycolide)
PVA – poly(vinyl alcohol)
MPs – microparticles

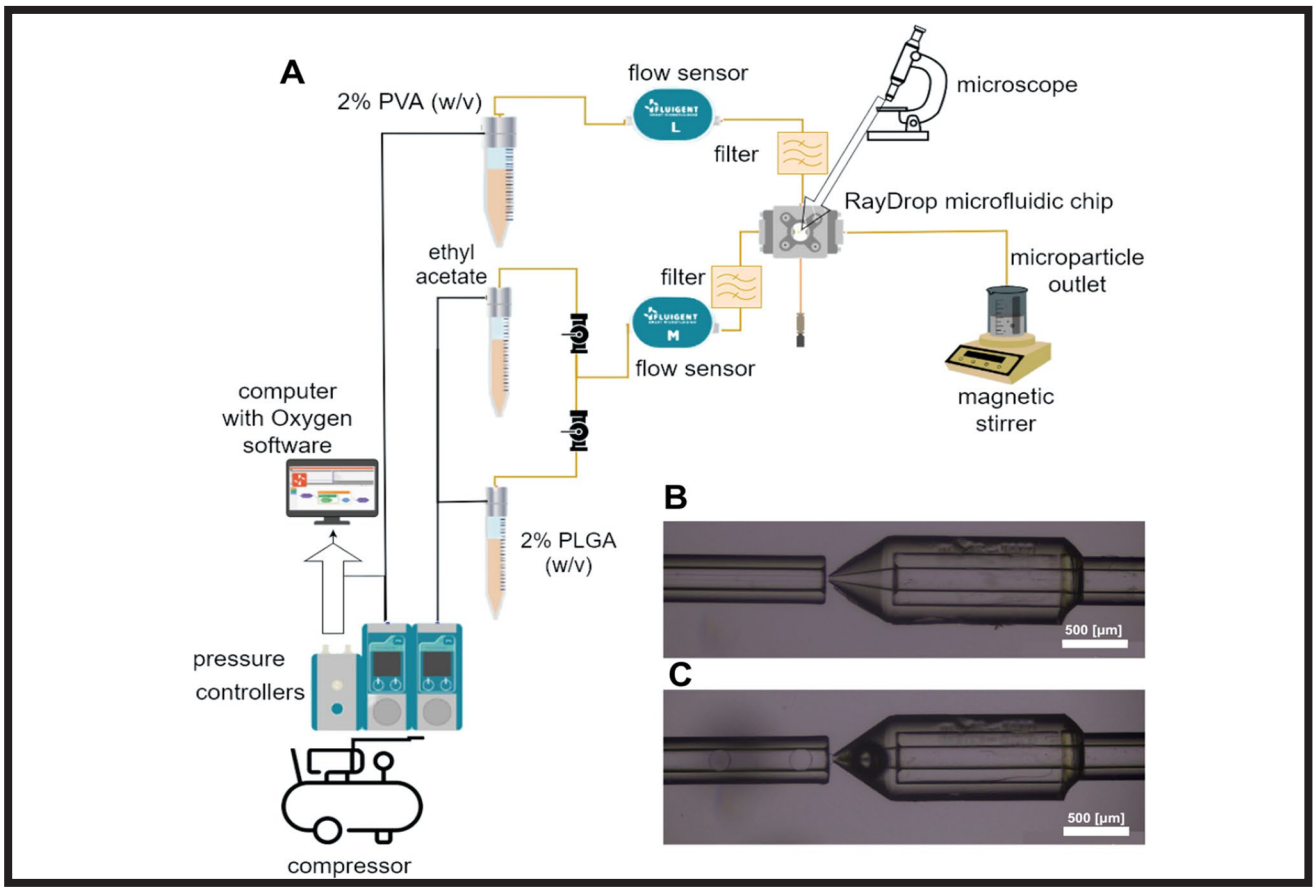

FIG. 2. Scheme of a microfluidic device RayDrop with accessories (adapted from [12]) (A); phase flow regime inside the RayDrop chip chamber during manufacturing of PLGA microparticles in jetting regime (B) and in dripping regime (C).

Microscopic observations

The MPs morphology was assessed with an optical microscope (Axiovert, Zeiss, magnification: 75X), and ImageJ software was used to measure the size of microparticles (n = 50).

In vitro studies

The MPs were sterilized by immersion in 70% ethanol for 24 h and irradiated with a UV lamp for 30 min. MG-63 osteoblast-like cells (ATCC® CCL-1™, American Type Culture Collection) were cultured in minimal essential medium (MEM, PAN BIOTECH) in contact with MPs on a 24-well plate (Avantor, VWR) at 37°C and 5% CO_2. For each of the well, 2 mg MPs and 500 µl of cell suspension in MEM (16 000 cells/ml) were added and cells were cultured for 1 and 3 days. During incubation, the culture plates were placed on a shaker (PS-3D Sunflower Mini-Shaker, Grant Instruments), with a speed of 30 rpm, to ensure dynamic conditions.

Cell viability was tested with resazurin reduction and live-dead fluorescence staining. The metabolic activity AlamarBlue test (resazurin-based, Sigma-Aldrich) was carried out using 5% resazurin solution; 300 µl of the solution was added to each of the wells, then incubated for 2 h at 37°C, 5% CO_2. The solution was then transferred to a black 96-well plate (Nunc), and fluorescence was measured at an excitation wavelength of 544 nm and an emission wavelength of 590 nm (FluoStar Omega, BMG Labtech). The percentage of resazurin reduction was calculated using the formula (1):

$$\%\text{Rezasurin Reduction} = 100\% \cdot \frac{F_s - F_c}{F_{100\%} - F_c} \qquad (1)$$

where F_s – fluorescence of the sample, F_c – fluorescence of 5% of AlamarBlue solution in a cell-free medium, $F_{100\%}$ – fluorescence of 5% of AlamarBlue solution in a medium after complete reduction at 120°C for 15 min.

In order to assess the arrangement of cells around the MPs and to distinguish between live and dead cells, live/dead staining was performed. This test consisted of adding 300 µl of 0.1% propidium iodide (Sigma Aldrich) and 0.1% calcein AM (Sigma Aldrich) solution in PBS to the wells, then incubated in the dark for 10 min. Subsequently, cells were observed under a fluorescent microscope (Axiovert 40 CFL, Zeiss).

Statistical analysis

The obtained data were checked for normal distribution, the Shapiro-Wilk and Lilliefors test were used. In addition, quantile-quantile plots were prepared. Then, the mean, the standard deviation (SD), and the coefficient of variation (CV) were calculated. The CV is a statistical measure that allows to assess the variability of data in relation to the mean. It is particularly useful when comparing data sets with different means. It was calculated from the formula (2):

$$CV = \frac{SD}{\bar{X}} \cdot 100\% \qquad (2)$$

where: CV – coefficient of variation, SD – standard deviation and $\bar{X}$ – mean.

All calculations and statistical analysis were performed using OriginPro 2023b software.

Results and Discussion

Properties of microparticles

The results show that for each of the PVA concentrations in the water phase, as the PLGA concentration increased, the size of the MPs also increased. As detailed in TABLE 1 and FIG. 3, the highest MPs diameters, equal to 133.5 ± 27.2 µm, were found for microparticles produced when PVA concentration in the water phase was 5% and PLGA concentration in the oil phase was 4%. The smallest MPs, equal to 35.9 ± 9.2 µm, were formed when they were produced with the use of 0.5% PVA in the water phase and 1% PLGA in the oil phase.

TABLE 1. Summary of PLGA MPs size obtained by emulsification by mixing; SD – standard deviation, CV – coefficient of variation.

PVA concentration [%]	PLGA concentration [%]	Mean [µm]	SD [µm]	CV [%]
0.5	1	35.9	9.2	31
	2	56.7	10.8	26
	4	126.0	22.2	25
1	1	48.9	17.3	39
	2	69.7	11.1	24
	4	99.2	30.7	35
2	1	42.6	9.2	28
	2	64.5	12.4	26
	4	90.8	19.4	28
2.5	1	74.6	15.3	27
	2	79.6	25.2	36
	4	98.3	16.3	25
4	1	70.4	23.6	37
	2	87.7	20.2	29
	4	121.7	22.5	26
5	1	60.6	11.9	27
	2	77.9	25.6	37
	4	133.5	27.2	27

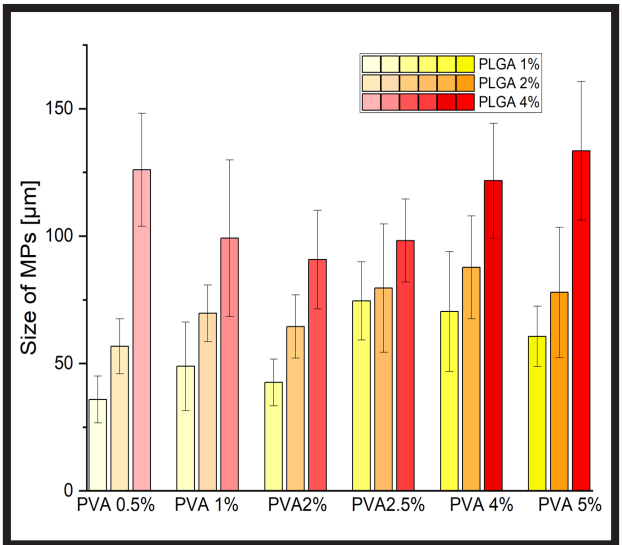

FIG. 3. Sizes of MPs obtained by single emulsification by mixing: the concentration of PLGA in the oil phase was 1%, 2% and 4%, while the concentration of PVA in the water phase was 0.5%, 1%, 2%, 2.5%, 4% and 5%.

The coefficient of variation in MPs diameters was between 24% and 39%, which shows that using the emulsification method by mixing, microparticles with a large but reproducible dispersion can be obtained.

Using the microfluidic device, the sample was obtained using a 2% PVA solution in the water phase and a 2% PLGA solution in the oil phase. The mean diameter of MPs was equal to 43.2 ± 3.2 μm, and the coefficient of variation was 7%, which was the lowest result of all microparticles obtained during the study. The MPs produced in the microfluidic device were characterized by a smaller size and a lower polydispersity as compared to those produced by batch emulsification.

The size of the MPs obtained with the microfluidic device was 43.2 ± 3.2 μm, which was similar to the MPs with 42.6 ± 9.2 μm size obtained with 1% PLGA concentration in the oil phase and 2% PVA concentration in the water phase. Therefore, these two sample types were selected for *in vitro* studies, and their size with standard deviation is presented in FIG. 4A.

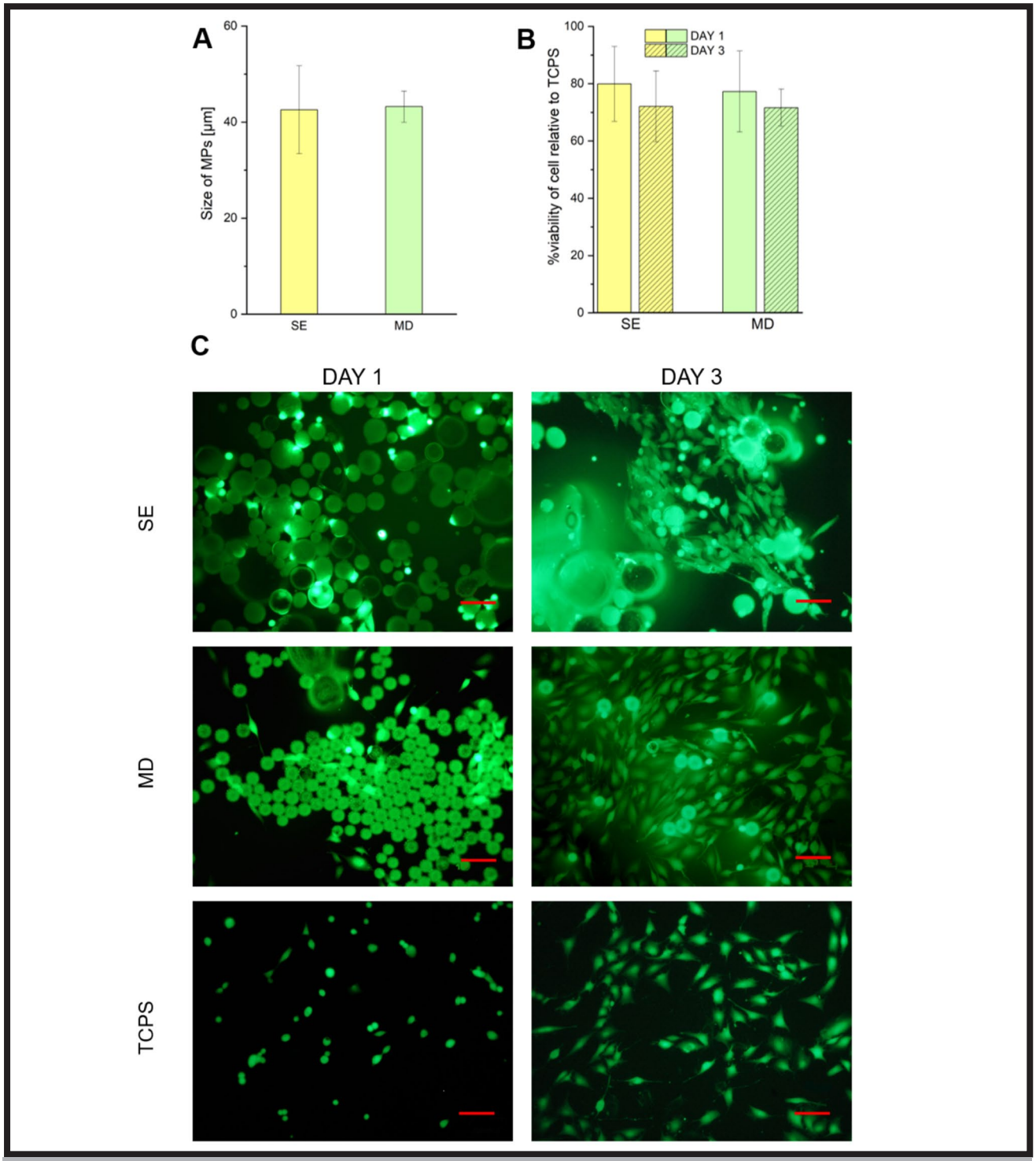

FIG. 4. Size of MPs used in in vitro studies (A); AlamarBlue test results, cell viability relative to control TCPS samples (B); Live/dead staining results after day 1 and day 3: SE – single emulsification, MD – microfluidic device, TCPS – tissue culture polystyrene control sample, scale bar = 100 μm (C).

***In vitro* studies**

To assess the suitability of the materials in the context of bone tissue engineering, *in vitro* studies were conducted. AlamarBlue test showed that for the MPs samples studied in contact with MG-63 cells, cell growth was in the range of 70-80% of control conditions (cells cultured on tissue culture polystyrene, TCPS) (FIG. 4B). Interestingly, in our experiment carried out for the TCPS control sample, the measured resazurin reduction ranged from 2.30% to 2.56%. As shown in our previous studies for a similar number of seeded MG-63 cells, but in static conditions, the resazurin reduction on day 1 was approximately 15-25% and on day 3 it was approximately 30% [13-15]. Lower proliferation in the experiment reported here may be the result of the dynamic culture conditions, because the culture plates were placed on the shaker, which was expected to provoke cell aggregation around microparticles. Nevertheless, it has been shown that MPs produced by emulsification and using a microfluidic device had a similar effect on MG-63 cell viability and are cytocompatible, according to ISO 10993-5 [16].

The viability of cells was confirmed by live/dead staining (FIG. 4C). It was found that after day 1 and 3, the cells grew normally for the control sample and they were stained green, thus alive. For both types of MPs, cells were clustered around the MPs. However, in the areas where the MPs were too dense and the cells did not have space to grow, no cells were observed. Interestingly, no dead red-stained cells were seen, which means that the MPs were not cytotoxic.

Conclusions

PLGA microparticles were obtained with emulsification by mixing and by using a microfluidic device. The microparticles were characterized taking into account their diameter and coefficient of variation. It was shown that the size of microparticles can be controlled by the concentration of PLGA in the oil phase: the higher the concentration, the larger the size. Interestingly, increased concentration of PVA in the water phase has a minor effect on particle size. The MPs obtained by mixing are more polydispersed (coefficient of variation between 24% and 39%), in contrast to those produced using a microfluidic device, which had a coefficient of only 7%. It means that the microparticles produced using the microfluidic device are more homogenous in size. *In vitro* studies of the obtained materials were carried out under dynamic conditions, which significantly reduced MG-63 cells proliferation, but allowed the cellular aggregates to be obtained around the MPs. Viability tests showed that cells seeded on larger particles proliferate better than those seeded on smaller particles. PLGA MPs were found to be cytocompatible with osteoblast-like cells, as shown by the resazurin reduction test and live/dead staining.

Acknowledgements

This study was supported from the subsidy (No 16.16.160.557) for the AGH University of Krakow.

ORCID iD

S. Marecik: https://orcid.org/0009-0009-7729-424X
M. Krok-Borkowicz: https://orcid.org/0000-0002-9415-0282
E. Pamuła: https://orcid.org/0000-0002-0464-6189

References

[1] Liu Z., Yuan X., Liu M., Fernandes G., Zhang Y., Yang S., Ionita C.N., Yang S.: Antimicrobial Peptide Combined with BMP2-Modified Mesenchymal Stem Cells Promotes Calvarial Repair in an Osteolytic Model. Molecular Therapy 26(1) (2018) 199-207. https://doi.org/10.1016/j.ymthe.2017.09.011

[2] Kang Y., Jabbari, E., Yang Y.: Integrating Top-Down and Bottom-Up Scaffolding Tissue Engineering Approach for Bone Regeneration. In: Micro and Nanotechnologies in Engineering Stem Cells and Tissues, 1st ed., Ramalingam M., Jabbari E., Ramakrishna S., Khademhosseini A. Eds. Wiley (2013) 142-158. https://doi.org/10.1002/9781118574775.ch6.

[3] Schmidt T., Xiang Y., Bao X., Sun T.: A Paradigm Shift in Tissue Engineering: From a Top–Down to a Bottom–Up Strategy. Processes 9(6) (2021) 935. https://doi.org/10.3390/pr9060935.

[4] Nichol J.W., Khademhosseini A.: Modular tissue engineering: engineering biological tissues from the bottom up. Soft Matter 5(7) (2009) 1312-1319. https://doi.org/10.1039/b814285h.

[5] Jin S., Xia X., Huang J., Yuan C., Zuo Y., Li Y., Li J.: Recent advances in PLGA-based biomaterials for bone tissue regeneration. Acta Biomater. 127(2021) 56-79. https://doi.org/10.1016/j.actbio.2021.03.067.

[6] Martins C., Sousa F., Araújo F., Sarmento B.: Functionalizing PLGA and PLGA Derivatives for Drug Delivery and Tissue Regeneration Applications. Adv Healthc Mater. 7(1) (2018). https://doi.org/10.1002/adhm.201701035.

[7] Kim G., Gavande V., Shaikh V., Lee W-K.: Degradation Behavior of Poly(Lactide-Co-Glycolide) Monolayers Investigated by Langmuir Technique: Accelerating Effect. Molecules. 28(12) (2023) 4810. https://doi.org/10.3390/molecules28124810

[8] Mielan B., Sousa D.M., Krok-Borkowicz M., Eloy P., Dupont C., Lamghari M., Pamuła E.: Polymeric Microspheres/Cells/Extracellular Matrix Constructs Produced by Auto-Assembly for Bone Modular Tissue Engineering. Int J Mol Sci. 22(15) (2021) 7897. https://doi.org/10.3390/ijms22157897

[9] Mielan B., Pamuła E.: Optimizing manufacturing conditions of polymer microspheres as cell carriers for modular tissue engineering. Eng.Biomat. 156 (2020) 2-9. https://doi.org/10.34821/eng.biomat.156.2020.2-9

[10] Lin Z., Wu J., Qiao W., Zhao Y., Wong K.H.M., Chu P.K., Bian L., Wu S., Zheng Y., Cheung K.M.C., Leung F., Yeung K.W.K.: Precisely controlled delivery of magnesium ions thru sponge-like monodisperse PLGA/nano-MgO-alginate core-shell microsphere device to enable in-situ bone regeneration. Biomaterials. 174 (2018) 1-16. https://doi.org/10.1016/j.biomaterials.2018.05.011.

[11] Li W., Zhang L., Ge X., Xu B., Zhang W., Qu L., Choi C.H., Xu J., Zhang A., Lee H., Weitz D.A.: Microfluidic fabrication of microparticles for biomedical applications. Chem Soc Rev. 47(15) (2018) 5646-5683. https://doi.org/10.1039/c7cs00263g.

[12] Fluigent. Microfluidic Droplet Production Method [online]. https://www.fluigent.com/resources-support/expertise/expertise-reviews/droplet-and-particle-generation-in-microfluidics/microfluidic-droplet-production-method. Accessed: Jun. 21, 2023.

[13] Pudełko I., Moskwik A., Kwiecień K., Kriegseis S., Krok-Borkowicz M., Schickle K., et al. Porous Zirconia Scaffolds Functionalized with Calcium Phosphate Layers and PLGA Nanoparticles Loaded with Hydrophobic Gentamicin. International Journal of Molecular Sciences 24(9) (2023) 8400. https://doi.org/10.3390/ijms24098400

[14] Rumian Ł., Wolf-Brandstetter C., Rößler S., Reczyńska K., Tiainen H., Haugen H.J., Scharnweber D., Pamuła E.: Sodium alendronate loaded poly(l-lactide- *co*-glycolide) microparticles immobilized on ceramic scaffolds for local treatment of bone defects. Regenerative Biomaterials 8(3) (2021) rbaa012. https://doi.org/10.1093/rb/rbaa012

[15] Cichoń E., Czechowska J.P., Krok-Borkowicz M., Allinson S.L., Stępień K., Smith A., Pamuła E., Douglas T.E.L., Zima A.: Biosurfactants as foaming agents in calcium phosphate bone cements. Biomaterials Advance 145 (2023) 213273. https://doi.org/10.1016/j.bioadv.2022.213273

[16] ISO 10993-5:2009. Biological evaluation of medical devices. Part 5: Tests for in vitro cytotoxicity.

ANTIBACTERIAL FABRICS MODIFIED WITH BETULIN FOR MEDICAL AND GENERAL APPLICATIONS

Artur D. Sowiński[1,2*], Ludwik A. Tarachowicz[2], Anna Kłeczek[1], Natalia Brzezińska[1], Maciej Pyza[1], Jadwiga Gabor[1], Zuzanna Gierek[3], Adam Zabrowarny[2,4], Andrzej S. Swinarew[1,5*]

[1] Faculty of Science and Technology, University of Silesia, 75 Pułku Piechoty 1A, 41-500 Chorzów, Poland
[2] Development Department, Partner Systems Sp. z o.o., Jerzego z Dąbrowy 5d, 77-300 Człuchów, Poland
[3] Faculty of Medical Sciences, Medical University of Silesia, Medyków 18, 40-752 Katowice, Poland
[4] Mechatronics Department, Kazimierz Wielki University in Bydgoszcz, Jana Karola Chodkiewicza 30, 85-064 Bydgoszcz, Poland
[5] Institute of Sport Science, The Jerzy Kukuczka Academy of Physical Education, Mikołowska 72A, 40-065 Katowice, Poland
*e-mail: artur.sowinski@us.edu.pl; andrzej.swinarew@us.edu.pl

Abstract

This study examines the potential use of betulin as an alternative to silver in enhancing vinyl-coated fabrics. Silver, commonly used to impart antimicrobial properties to polymers, raises environmental and cytotoxicity concerns. Betulin, known for its antibacterial, anti-inflammatory, antiviral, and antifungal characteristics, emerges as an eco-friendly alternative. The study highlights the possible applications of betulin in various sectors, such as medical, military, and public settings, where addressing the challenge of harmful biofilms is critical. The aim of this research was to assess the possible effectiveness of betulin as a modifier in polyvinyl chloride (PVC) coated textiles. The study involved extracting betulin, preparing plasticizer-based betulin premix, incorporating it into plastisol, and then coating fabrics to analyze its effect on surface bioactivity. Preliminary tribological studies were conducted to assess the durability of the coating. According to the ISO 22196:2007 standard, significant antibacterial effects were observed, with an activity rating (R) ranging between 1.55 and 2.0. In addition, tribological studies indicated an improvement in coating durability compared to conventional PVC coatings. The results suggest that betulin shows potential as a cost-efficient and environmentally friendly alternative, contributing to improved product functionality while minimizing environmental impact. Further research is planned to investigate the potential of betulin in polymer modification and to exploit its positive impact on human health and environmental sustainability.

Keywords: *betulin, antimicrobial fabrics, biofilm prevention, polyvinyl chloride coating, activity rating, tribological studies*

[Engineering of Biomaterials 169 (2023) 23-26]

doi:10.34821/eng.biomat.169.2023.23-26

Submitted: 2023-07-25, Accepted: 2023-08-22, Published: 2023-08-25

Introduction

The modification of synthetic materials is an important aspect in the design of polymers with specific properties. The continuous exploration of new modifiers and methods is essential to achieve the desired material characteristics.

In order to enhance the antimicrobial properties of synthetic materials, a common practice is to make modifications by incorporating silver ions into the chemical composition [1]. The antibacterial activity of these modified polymers is dependent on the release of silver ions. However, it has been observed that these ions exhibit cytotoxic effects on living organisms, and their release can potentially lead to environmental sterilization [2].

An innovative approach to modifying synthetic materials appears to be the application of betulin, a natural and organic compound derived from the white bark of birch trees. Betulin is a substituted triterpene (FIG. 1) with highly valuable properties, demonstrating antibacterial, anti-inflammatory, antiviral, and even antifungal activities [2,3]. This compound is an economical alternative to silver ions, as its production cost is relatively lower. Betulin has a vide range of applications in various fields. In addition to its antibacterial, antiviral and anti-inflammatory effects, birch bark extract exhibits antioxidant and even anticancer properties [4]. It may also be useful in personal protection, serving as a modifier in the chemical composition of respiratory masks for upper respiratory tract protection [5].

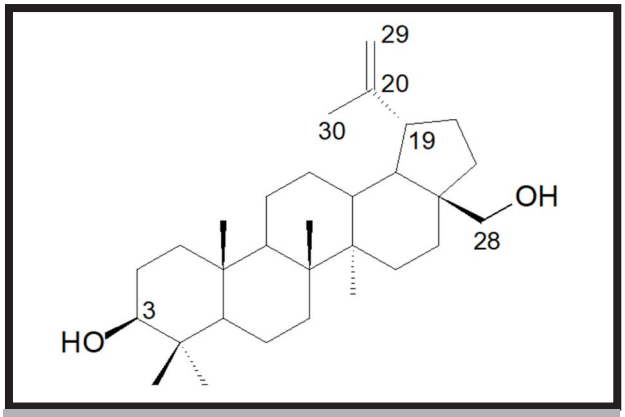

FIG. 1. Chemical formula of betulin [2].

In the context of current technological developments, fabrics containing betulin as a coating are not yet widely available on the market. Current practice is dominated by fabrics coated with PU (polyurethane), PA (polyamide) or PES (polyester), DWR (Durable Water Repellent), and microporous coatings, or Kevlar fabrics [6-8]. However, such materials do not fully meet the requirements for military and civilian applications because they lack the microbiological activity crucial for protection against harmful biofilm formation. It is important to note that each type of fabric has its own characteristic features that determine its suitability for specific implementations.

The aim of this study was to evaluate the potential utility of betulin as a modifier in textiles coated with polyvinyl chloride (PVC). This compound facilitates the integration of coated fabric structures with a natural extract, allowing the assessment of its impact on the final product. Such an enhancement of the product could improve its functional qualities and allow for the elimination of problematic, commonly used modifiers. The study also investigated the influence of betulin on the bioactivity of the surface. Preliminary tribological evaluation was performed as well.

Materials and Methods

In this experiment, a 500D polyester fabric, with a density of 15 fibers/cm^2 (15x15) was used as the base material. Plastisol (PVC + plasticizer + modifiers) with a composition identical to the reference sample was used for modification, incorporating 1% betulin.

The first step was to extract betulin from the birch bark using the Soxhlet extraction method (FIG. 2a). In order to combine the obtained active substance with plastisol, it was necessary to process the extract appropriately. For this purpose, a plasticizer-based betulin premix was prepared to increase affinity and facilitate homogenization. The active ingredient was extracted from the alcohol-based extract (FIG. 2b), and then the dry mass was grated in a mortar together with the plasticizer (FIG. 3a). In the next stage, the prepared mixture could easily be introduced into the plastisol used in the experiment (FIG. 3b).

After incorporating the active substance into the mixture and seasoning the modified paste, the process of producing an experimental coated fabric was initiated using blade coating technology under laboratory conditions (FIG. 4a). Subsequently, a sample fabric was produced (FIG. 4b) and subjected to further examinations. The parameters and details of the fabric production process are proprietary knowledge of the Partner Systems Sp. z o.o. company.

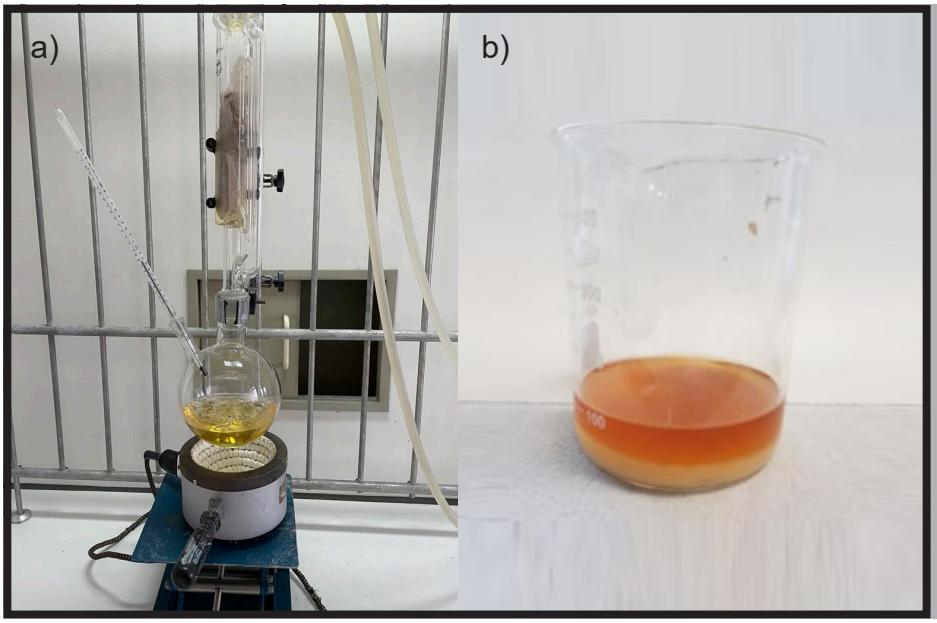

FIG. 2. Extraction of betulin in a Soxhlet apparatus (a) and obtained alcohol-based betulin extract (b).

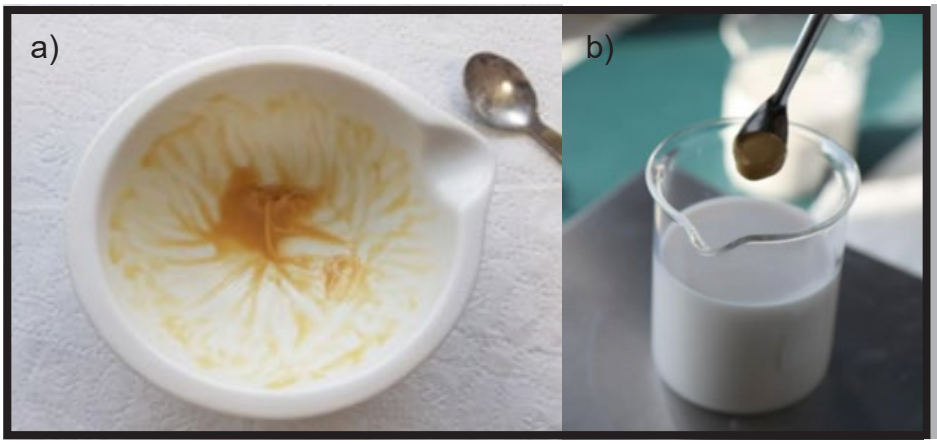

FIG. 3. Plasticizer-based betulin premix (a) and its addition to plastisol (b).

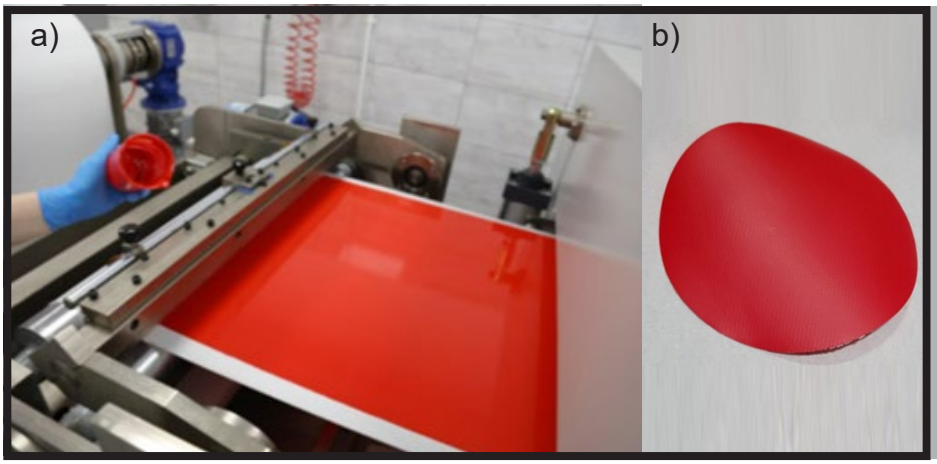

FIG. 4. The fabric coating process (a) and a cutout of the resulting coated fabric sample (b).

TABLE 1. Parameters of the microbiological activity tests.

Research standard	ISO 22196:2007(E) "Plastics - Measurement of antibacterial activity on plastics surfaces"
Type of plastic used for control samples (size, shape, thickness)	50 mm x 50 mm x 1 mm
Type of plastic used for test samples (size, shape, thickness)	50 mm x 50 mm x 1 mm
Type of polymer used as "cover film" (size, shape, thickness)	PP film, 40 mm x 40 mm, 0.05 mm
Bacterial species and type of strain used	*Escherichia coli* - DSM 1576; *Staphylococcus aureus* DSM 346
Inoculum volume	0.4 ml
Concentration of bacteria in inoculum	6 x 10^5 cells/ml
Volume, type of neutralizer	10 ml, SCDLP broth

The assessment of the antibacterial activity of the obtained polymeric materials was carried out in accordance with the ISO 22196:2007 (E) standard "Plastics - Measurement of antibacterial activity on plastic surfaces" (TABLE 1). *Escherichia coli* DSM 1576 and *Staphylococcus aureus* DSM 346 were used as the reference strains. The bacterial inoculum had a volume of 0.4 ml with a concentration of 6 x 10^5 bacteria/ml. The samples were incubated at a temperature of 35°C with a humidity level of at least 90% for 24 h. Each sample was neutralized following the procedures described in the standards PN ISO 18593:2005 and PN ISO 14562:2006. After the samples were subjected to a sequence of 10-fold dilutions, they were placed in Petri dishes and incubated as specified in the standard. The N coefficient, which represents the number of live bacteria recovered per cm^2 of the sample, was calculated for both test and control samples. For antibacterial tests, the coated fabric without betulin served as the reference sample. Three reference samples for each strain, along with three samples of material containing 1% betulin, were used for the study.

The average antibacterial activity (R) for the assessed fabric was calculated based on:

$$R = (U_t - U_0) - (A_t - U_0) = U_t - A_t$$

where:
U_0 – the average decimal logarithm of the count of viable bacteria (cells/cm^2), retrieved from untreated samples after inoculation;
U_t – the average decimal logarithm of the count of viable bacteria (cells/cm^2), retrieved from untreated samples after 24 h;
A_t – the average decimal logarithm of the count of viable bacteria (cells/cm^2), retrieved from treated samples after 24 h.

Subsequently, tribological tests were conducted to assess the impact of the examined extract on the surface of the coated fabric, as well as to determine the average coefficient of friction (μ). All samples were tested on a standard tribometer (Anton-Paar, Corcelles-Cormondrèche, Switzerland) under identical conditions: temperature 21°C, air atmosphere, humidity 40%. The test parameters were as follows: sequence count 1; single-way mode; radius 5.99 mm; linear speed 10 cm/s; acquisition rate 20 Hz; normal load 5 N. The samples used for the tribological tests included the reference sample, three samples containing 1% betulin, and the coated fabric sample with betulin sprayed on the surface.

Results and Discussions

TABLE 2 presents the results of the microbiological activity tests conducted on the surface of the coated fabric. The parameters U_0, U_t, and A_t, together with the calculated antibacterial activity denoted as R (1.85), provide insight into the antibacterial properties of the fabric.

The derived antibacterial activity R (1.85) obtained from the tests, indicates a moderate level of antibacterial efficacy for the betulin-modified fabric. This value falls within the range of 1.5 to 2.0, as shown in TABLE 3, corresponding to an acceptable level of bacteriostatic activity according to the ISO 22196:2007 standard. These findings underscore the potential of betulin as a promising alternative to silver-based modifiers in fabric modification processes, suggesting its capacity to enhance microbial resistance in polyvinyl chloride-coated textiles.

TABLE 2. Results of the microbiological activity tests.

Parameter	Measured value
U_0	4.21
U_t	4.91
A_t	3.46
Antibacterial activity - R	1.85

TABLE 3. Assessment of antibacterial effectiveness.

Antibacterial efficacy R according to ISO 22196:2007	Number of killed bacteria [%]	Assessment
< 1.5	< 96.8	Poor
1.5 - 2.0	96.8 - 99.0	Acceptable
2.0 - 3.0	99.0 - 99.9	Good
> 3.0	> 99.9	Excellent

TABLE 4 shows the test results of the reference materials using *Staphylococcus aureus* and *Escherichia coli* bacteria. The presence of bacterial growth observed in both cases underscores the imperative for antimicrobial intervention in fabric modification processes to mitigate pathogenic proliferation effectively.

TABLE 5 presents preliminary results of the tribological tests of coated fabric samples, elucidating the influence of betulin content on the coating strength and the average coefficient of friction (μ) to damage the coating. The results indicate a noticeable enhancement in coating strength in the betulin-modified samples compared to the reference sample, suggesting the potential of betulin in reinforcing coating durability. These findings substantiate the effectiveness of betulin as a modifier in improving both product functionality and durability.

Betulin-modified fabrics possess significant potential for use in many sectors, including military and civilian applications, due to their inherent ability to provide robust protection against harmful biofilms and pathogens. Additionally, these fabrics offer a sustainable solution by minimizing the environmental impact, attributed to the ecofriendly nature of the betulin derivatives used in their modification.

TABLE 4. Growth of *Staphylococcus aureus DSM 346, Escherichia coli* DSM 1576.

Validation conditions	*Staphylococcus aureus* DSM 346	*Escherichia coli* DSM 1576
(Lmax - Lmin) / Lmean ≤ 0.2	0.17	0.17
Average number of bacterial colonies covering the control sample immediately after inoculation 6.2×10^3 CFU/cm^2 : 2.5×10^4 CFU/cm^2	1.0×10^4 CFU/cm^2	9.2×10^3 CFU/cm^2
The average number of bacterial colonies covering the control sample after 24 h ≥ 6.2×10^1 CFU/cm^2	1.2×10^5 CFU/cm^2	3.1×10^5 CFU/cm^2
Validation conditions:	Fulfilled	Fulfilled

TABLE 5. Preliminary results of the tribological tests.

	Average coating strength [m]	Average coefficient of friction μ to damage the coating
Reference sample	4.52	0.579
Betulin contents 1% by mass sample (1,2,3)	26.17	0.645
Coated fabric sample with betulin (sprayed on the surface)	13.10	0.651

Conclusions

Birch bark-derived betulin is a promising eco-friendly alternative to silver in modifying vinyl-coated fabrics, offering antibacterial properties without environmental or cytotoxicity concerns.

The microbiological study demonstrates the effectiveness of betulin-modified polyvinyl chloride (PVC) coated textiles in inhibiting bacterial growth, as indicated by an activity rating (R) ranging from 1.55 to 2.0, meeting acceptable antibacterial efficacy standards.

Tribological evaluations demonstrate increased durability of coatings compared to conventional silver-based counterparts, thus explaining betulin's latent ability to enhance both functional effectiveness and product durability.

Betulin-modified fabrics have potential applications in military, medical, and public settings, providing protection against harmful biofilms and pathogens while minimizing environmental impact.

As a result, it has been concluded that further research on combining the beneficial properties of betulin with the practical aspect of coated fabrics is warranted.

Acknowledgements

The work was carried out as part of the statutory research of the Institute of Biomedical Engineering, University of Silesia.

ORCID iD

A.D. Sowiński: https://orcid.org/0009-0006-4922-6790
L.A. Tarachowicz: https://orcid.org/0009-0008-2059-2177
A. Kłeczek: https://orcid.org/0000-0001-6066-3349
N. Brzezińska: https://orcid.org/0000-0002-8648-2498
M. Pyza: https://orcid.org/0000-0002-7904-9303
J. Gabor: https://orcid.org/0000-0003-4850-1608
Z. Gierek: https://orcid.org/0009-0004-2107-9755
A. Zabrowarny: https://orcid.org/0000-0002-4252-4967
A.S. Swinarew: https://orcid.org/0000-0001-6116-9510

References

[1] Osonga F.J., Kariuki V.M., Yazgan I. et al.: Synthesis and antibacterial characterization of sustainable nanosilver using naturally-derived macromolecules. Sci Total Environ 563-564 (2016) 977-986.
[2] Swinarew A., Boryczka S., Mazurek U. et al.: Modyfikowany polimer termoplastyczny o właściwościach przeciwbakteryjnych i przeciwzapalnych oraz sposób jego otrzymywania, Polska, 422092 B1, 03.07.2017.
[3] Jasicka-Misiak I., Lipok J., Świder I.A., Kafarski P.: Possible fungistatic implications of betulin presence in betulaceae plants and their hymenochaetaceae parasitic fungi. Z Naturforsch C J Biosci 65 (3-4) (2010) 201-206.
[4] Malinowska M., Sikora E., Ogonowski J.: Ekstrakt z brzozy brodawkowatej Cortex Betulae, jako źródło substancji aktywnych. Herbalism 1(5) (2019) 17-31.
[5] Brzezińska N., Pyza M., Kłeczek A. et al.: Fabrication of filter membrane of organic compound to protect the upper respiratory tract from viral and bacterial infections, including SARS-Cov-2, compliant with FFP2 standard. Engineering of Biomaterials 166 (2022) 2-11.
[6] Aldalbahi A., El-Naggar M.E., El-Newehy M.H. et al.: Effects of Technical Textiles and Synthetic Nanofibers on Environmental Pollution. Polymers 13(1) (2021) 155.
[7] Byrne C.: Technical textiles market - An overview. In: Horrocks A.R., Anand A.R. (eds), Handbook of Technical Textiles. Woodhead Publishing (2000) 1-23.
[8] Revaiah R.G., Kotresh T.M., Kandasubramanian B.: Technical textiles for military applications. J. Text. Inst. 111(2) (2020) 273-308.